Lithos xxx (2013) xxx

Contents lists available at ScienceDirect

Lithos

journal homepage: www.elsevier.com/locate/lithos

Highlights

Lithos xxx (2013) xxx–xxx

Origin of basaltic magmas of Perşani volcanic field, Romania: A combined whole rock and mineral scale investigation

Szabolcs Harangi [a,b], Tamás Sági [a,b], Ioan Seghedi [c], Theodoros Ntaflos [d]

[a] MTA-ELTE Volcanology Research Group, Pázmány sétány 1/C, H-1117 Budapest, Hungary
[b] Department of Petrology and Geochemistry, Eötvös University, Pázmány sétány 1/C, H-1117 Budapest, Hungary
[c] Institute of Geodynamics, Romanian Academy, 19-21. str. Jean-Luis Calderon, 020032 Bucharest, Romania
[d] Department of Lithospheric Research, University of Vienna, Althanstrasse 14, A-1090 Vienna, Austria

- Integrated investigation of bulk rock and mineral compositional data of mafic rocks
- Origin of basaltic magmas in a low-volume flux monogenetic volcanic field
- Constrain on the mantle potential temperature and depth of melting column
- Subtle differences in the source region as shown by the composition of Cr-spinels
- Rapid magma ascent rate calculated from the Ca profile across olivine xenocrysts

http://dx.doi.org/10.1016/j.lithos.2013.08.025

Please cite this article as: Harangi, S., et al., Origin of basaltic magmas of Perşani volcanic field, Romania: A combined whole rock and mineral scale investigation, Lithos (2013), http://dx.doi.org/10.1016/j.lithos.2013.08.025

Lithos xxx (2013) xxx–xxx

Contents lists available at ScienceDirect

Lithos

journal homepage: www.elsevier.com/locate/lithos

Origin of basaltic magmas of Perşani volcanic field, Romania: A combined whole rock and mineral scale investigation

Szabolcs Harangi[a,b], Tamás Sági[a,b], Ioan Seghedi[c], Theodoros Ntaflos[d]

[a] MTA-ELTE Volcanology Research Group, Pázmány sétány 1/C, H-1117 Budapest, Hungary
[b] Department of Petrology and Geochemistry, Eötvös University, Pázmány sétány 1/C, H-1117 Budapest, Hungary
[c] Institute of Geodynamics, Romanian Academy, 19-21. str. Jean-Luis Calderon, 020032 Bucharest, Romania
[d] Department of Lithospheric Research, University of Vienna, Althanstrasse 14, A-1090 Vienna, Austria

ARTICLE INFO

Article history:
Received 16 April 2013
Accepted 29 August 2013
Available online xxxx

Keywords:
Alkaline basalt
Olivine
Chromian spinel
Monogenetic volcanic field
Magmagenesis
Carpathian–Pannonian region

ABSTRACT

The Perşani volcanic field is a low-volume flux monogenetic volcanic field in the Carpathian–Pannonian region, eastern-central Europe. Volcanic activity occurred intermittently from 1200 ka to 600 ka, forming lava flow fields, scoria cones and maars. Selected basalts from the initial and younger active phases were investigated for major and trace element contents and mineral compositions. Bulk compositions are close to those of the primitive magmas; only 5–12% olivine and minor spinel fractionation occurred at 1300–1350 °C, followed by clinopyroxenes at about 1250 °C and 0.8–1.2 GPa. Melt generation occurred in the depth range from 85–90 km to 60 km. The estimated mantle potential temperature, 1350–1420 °C, is the lowest in the Pannonian Basin. It suggests that no thermal anomaly exists in the upper mantle beneath the Perşani area and that the mafic magmas were formed by decompression melting under relatively thin continental lithosphere. The mantle source of the magmas could be slightly heterogeneous, but is dominantly variously depleted MORB-source peridotite, as suggested by the olivine and spinel composition. Based on the Cr-numbers of the spinels, two coherent compositional groups (0.38–0.45 and 0.23–0.32, respectively) can be distinguished that correspond to the older and younger volcanic products. This indicates a change in the mantle source region during the volcanic activity as also inferred from the bulk rock major and trace element data. The younger basaltic magmas were generated by lower degree of melting, from a deeper and compositionally slightly different mantle source compared to the older ones. The mantle source character of the Perşani magmas is akin to that of many other alkaline basalt volcanic fields in the Mediterranean close to orogenic areas. The magma ascent rate is estimated based on compositional traverses across olivine xenocrysts using variations of Ca content. Two heating events are recognized; the first one lasted about 1.3 years implying heating of the lower lithosphere by the uprising magma, whereas the second one lasted only 4–5 days, which corresponds to the time of magma ascent through the continental crust. The alkaline mafic volcanism in the Perşani volcanic field could have occurred as a response to the formation of a narrow rupture in the lower lithosphere, possibly as a far-field effect of the dripping of dense continental lithospheric material beneath the Vrancea zone. Upper crustal extensional stress-field with reactivation of normal faults at the eastern margin of the Transylvanian basin could enhance the rapid ascent of the mafic magmas.

1. Introduction

Monogenetic volcanic fields are clusters of individual small-volume, short-lived volcanic centers, which are the manifestation of the arrival of discrete magma batches from the upper mantle (Brenna et al., 2012; Németh, 2010). Magmas are thought to pass through the crust rapidly (Jankovics et al., 2013; Mattsson, 2012), often without significant modification of their geochemical composition; thus they provide invaluable information about their mantle sources and melt generation.

Basaltic monogenetic volcanic fields occur throughout the Mediterranean and surrounding regions (Beccaluva et al., 2011; Harangi et al., 2006; Lustrino and Wilson, 2007; Lustrino et al., 2011; Wilson and Bianchini, 1999). The composition of the basaltic rocks share many common features, yet their origin is still a subject of debate. Many of these volcanic fields occur spatially and temporally with calc-alkaline volcanic provinces (Lustrino et al., 2011) such as in the Betic–Rif–Tell system, Valencia trough, Sardinia, Provence, Southern Tyrrhenian area, Veneto, Carpathian–Pannonian region, Western Anatolia and the Aegean system. In spite of this, most of the basalts have similar compositional features to those found in western and central Europe and do not show any subduction-related signature (Lustrino and Wilson, 2007; Wilson and Downes, 1991). This indicates that the metasomatized mantle domain was successively replaced by upwelling fresh mantle material. Recently, Beccaluva et al. (2011) suggested that the alkaline basaltic volcanism in the Betics and Sardinia could be attributed to the far-field effect of slab

E-mail address: szabolcs.harangi@geology.elte.hu (S. Harangi).

0024-4937/$ – see front matter © 2013 Elsevier B.V. All rights reserved.
http://dx.doi.org/10.1016/j.lithos.2013.08.025

roll-back and the associated remobilization of deep mantle components. Using principally whole rock isotope and trace element data, they inferred that the primary magmas were formed in different parts of the lithospheric mantle, metasomatized by various fluids. In contrast, other authors have emphasized the sublithospheric origin of the basaltic magmas (e.g., Harangi and Lenkey, 2007; Lustrino and Wilson, 2007; Seghedi et al., 2004b).

In this paper we present the results of a combined whole-rock and mineral-scale study of the Quaternary (1.2–0.6 Ma; Panaiotu et al., 2013) alkali basalts in the Perşani Mts., SE-Carpathians, in order to constrain the origin of the basaltic magmas. This approach has been successfully applied to other volcanic centers of the Pannonian Basin (e.g., Ali and Ntaflos, 2011; Ali et al., 2013; Jankovics et al., 2012, 2013) and results in a better understanding of the magma plumbing systems beneath monogenetic volcanic fields, involving the nature of the mantle source region, melt generation and processes during magma ascent. The Perşani volcanic field is a low eruptive volume flux area (Valentine and Perry, 2007) and is the youngest volcanic area in the Carpathian–Pannonian region during the Late Miocene–Quaternary alkaline basalt volcanism (Downes et al., 1995; Embey-Isztin et al., 1993; Harangi, 2001a; Harangi and Lenkey, 2007; Seghedi and Szakács, 1994; Seghedi et al., 2004b). Eruption of basaltic magmas postdated the calc-alkaline volcanism in the Harghita Mts. (5.3–1.6 Ma; Pécskay et al., 1995) and was partly coeval with high-K calc-alkalic magmatism south of Harghita Mts. (Malnas–Bixad; 1–1.6 Ma) and predated the high-K calc-alkaline volcanism at Ciomadul (0.6–0.03 Ma; Pécskay et al., 1995; Harangi et al., 2010). The principal questions are what was the driving mechanism and the condition of the melt generation that lead to the formation of this localized, small-volume magmatic system, and how the alkali basaltic magmas could have formed close to a calc-alkaline to high-K calc-alkaline volcanic chain. These new results could also be significant in evaluating the present state of this volcanic field in an area that is still geodynamically active and could contribute to the understanding of the origin of such complex magmatic systems in the Mediterranean.

2. Geological setting

In the Carpathian–Pannonian region, a wide range of volcanic activity has taken place during the last 20 Ma (Harangi, 2001a; Harangi and Lenkey, 2007; Konečný et al., 2002; Seghedi and Downes, 2011; Seghedi et al., 2004a; Szabó et al., 1992). Alkaline basaltic volcanism occurred from 11 Ma to 0.1 Ma, forming monogenetic volcanic fields as well as scattered volcanic centers (Fig. 1A; Martin and Németh, 2004; Seghedi et al., 2004b; Harangi and Lenkey, 2007). The Bakony–Balaton Upland and the Nógrád–Gemer volcanic fields are characterized by a long lasting and intermittent volcanic activity from 8 Ma to 2.3 Ma and 6.5 Ma to 0.4 Ma, respectively (Pécskay et al., 2006; Wijbrans et al., 2007). Smaller basaltic volcanic fields are found in the western and southeastern part of this region with shorter lifetime (Styria, Little Hungarian Plain and Perşani, respectively; Balogh et al., 1994; Harangi et al., 1995; Panaiotu et al., 2004, 2013; Ali et al., 2013). Scattered volcanic centers are found in Burgenland (Ali and Ntaflos, 2011), around Stiavnica (Dobosi et al., 1995) and Lucareţ (Downes et al., 1995; Tschegg et al., 2010). Although this volcanic activity was fed dominantly by basaltic magmas, a huge

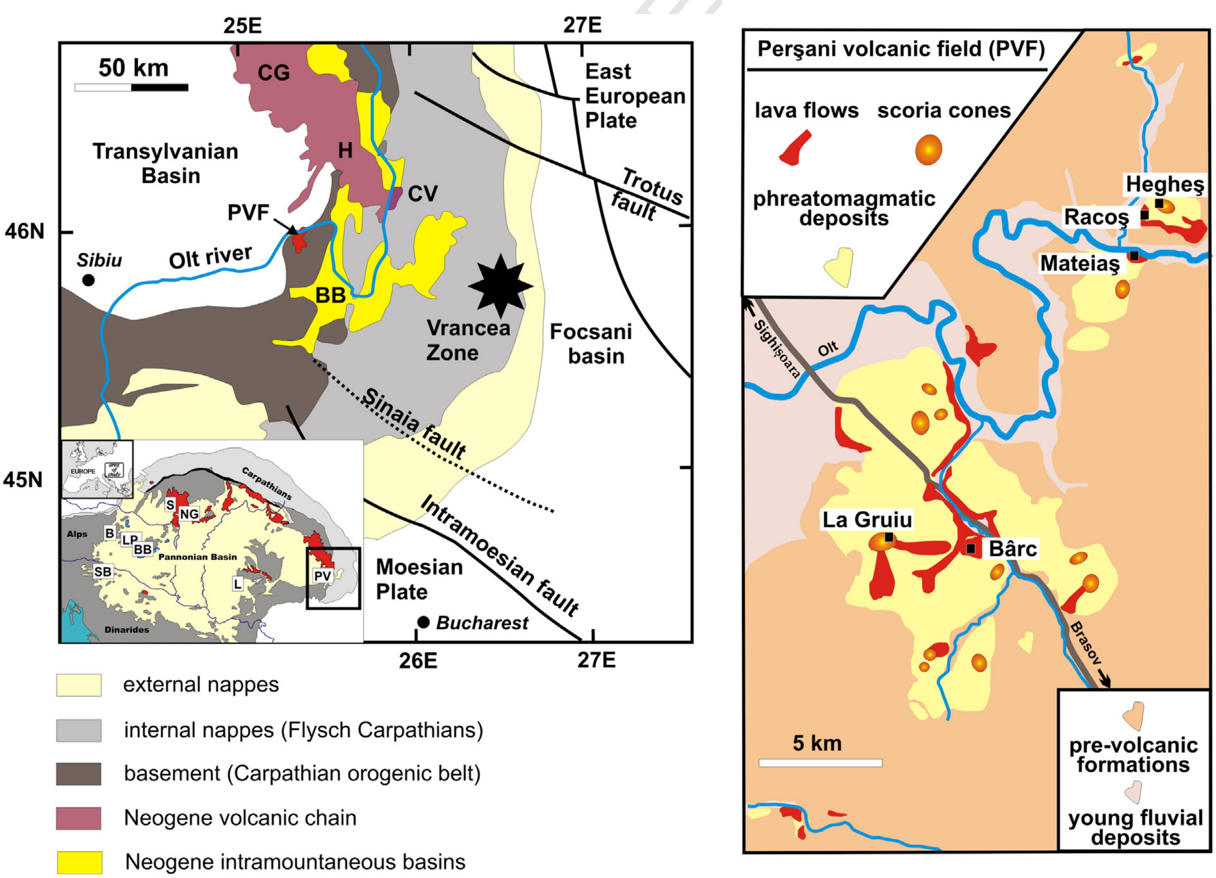

Fig. 1. A. Location of the Perşani Volcanic Field (PVF) in the southeastern Carpathian area of the Carpathian–Pannonian Region. CG = Călimani–Gurghiu volcanic complex, H = Harghita volcanic complex, CV = Ciomadul volcano; BB = Braşov basin. Inset: simplified map of the Carpathian–Pannonian Region with the monogenetic basalt volcanic fields: SB = Styrian Basin; B = Burgenland; LP = Little Hungarian Plain; BB = Bakony–Balaton Upland; S = Štiavnica; NG = Nógrád–Gemer; L = Lucareţ; PV = Perşani. B. Simplified volcanological map of the Perşani Volcanic Field after Szakács and Seghedi (1994) and Panaiotu et al. (2004, 2013) showing also the sample locations (black squares). Geological map after Cloetingh et al. (2004) and Martin et al. (2006).

Please cite this article as: Harangi, S., et al., Origin of basaltic magmas of Perşani volcanic field, Romania: A combined whole rock and mineral scale investigation, Lithos (2013), http://dx.doi.org/10.1016/j.lithos.2013.08.025

11–12 Ma old trachyandesite–alkaline trachyte volcano has been revealed at 2000 m depth in the basement of the Little Hungarian Plain that is genetically related to the basaltic volcanism (Harangi, 2001b; Harangi et al., 1995). The geodynamic relationships of the alkaline basaltic volcanism are still debated (Embey-Isztin et al., 1993; Harangi and Lenkey, 2007; Seghedi et al., 2004b). It took place during the post-extensional, thermal subsidence and partly the subsequent tectonic inversion stages (Horváth et al., 2006). In general, this kind of volcanic activity followed a widespread silicic and calc-alkaline volcanism in the Carpathian–Pannonian region; however, in detail the picture is more complex. The alkaline basaltic volcanism in the Styrian Basin followed potassic volcanism after a major time gap (1.9–3.9 Ma and 15–18 Ma, respectively; Pécskay et al., 2006). In the Nógrád–Gemer, the long-lasting alkaline basaltic volcanic activity spatially overlapped the calc-alkaline volcanic area and developed with continuous transition. In contrast, the Little Hungarian Plain and Bakony–Balaton Upland volcanic fields were formed without any connection to pre-existing calc-alkaline volcanism. In the southeastern part of this region, there is again a closer spatial–temporal relationship between the alkaline basaltic volcanic activity in Perşani and the calc-alkaline to high-K calc-alkalic volcanism (Seghedi et al., 2011). Here, eruptions of different magmas occurred partially contemporaneously.

The Perşani volcanic field is located at the southeastern part of the Carpathian–Pannonian Region (Fig. 1), just at the boundary between the Perşani Mts. and the Transylvanian basin, at the northwestern periphery of the intramontane Braşov basin (Fig. 1; Seghedi and Szakács, 1994; Gîrbacea et al., 1998; Ciulavu et al., 2000; Seghedi et al., 2011). This area is characterized by NE–SW trending normal faults, resulting from a NW–SE extensional regime (Gîrbacea et al., 1998). The eruptive centers appear to be structurally controlled and show a rough NE–SW trending alignment. The volcanism was coeval with post-collisional uplift in the Carpathian orogen and subsidence in the foreland area (Gîrbacea et al., 1998; Maţenco et al., 2007). Uplift of the Eastern Carpathians is still ongoing (1.5–2 mm/year; Cornea et al., 1979) accompanied with seismicity along the Trotuş and the Intramoesian faults (Fig. 1B). Extension and subsidence of the Braşov–Gheogheni basin system occurred contemporaneously with the highest uplift rate during Pliocene–Quaternary times (Gîrbacea and Frisch, 1998). A further important geodynamic element of this region is the Vrancea zone, where a sub-vertical seismically fast velocity slab has been detected (Oncescu et al., 1984). It exhibits the largest present-day strain concentration in continental Europe (Wenzel et al., 1999). Frequent earthquakes imply that this is still an active tectonic area, although the mechanism of the vertical slab formation and its geodynamic history is still unclear and highly debated. Possible scenarios involve the latest stage of subduction with ongoing slab-detachment (Martin et al., 2006; Sperner et al., 2001; Wortel and Spakman, 2000), delamination and roll-back of the lithospheric mantle (Chalot-Prat and Gîrbacea, 2000; Gîrbacea and Frisch, 1998) and removal of the lithospheric mantle as well as part of the lower crust beneath the overthickened collision zone (Fillerup et al., 2010; Koulakov et al., 2010). The Perşani volcanic field is underlain by relatively thick continental crust (35–40 km), whereas the thickness of the whole lithosphere is interpreted to be either thick (around 120 km; Dérerova et al., 2006; Horváth et al., 2006) or relatively thin (60–80 km; Martin et al., 2006; Seghedi et al., 2011). Popa et al. (2012) recorded subcrustal seismicity beneath the Perşani area and, using seismic tomography modeling, suggested that a low-velocity anomaly could be inferred at the crust–mantle boundary. This vertical low-velocity column could be interpreted as a magma ascent path or a set of magma reservoirs and would suggest that this area might be rejuvenated in the future and the possibility of further basaltic volcanic activity cannot be unambiguously excluded. The volcanic activity here occurred in a number of pulses between 1.2 Ma and 0.6 Ma (Panaiotu et al., 2004, 2013) and formed several volcanic centers (maars, scoria cones and lava flows) in a 22 km long and 8 km wide area (Seghedi and Szakács, 1994).

3. Samples and analytical techniques

Downes et al. (1995) investigated a set of basalts covering most of the eruptive centers in the Perşani volcanic field. For this study, we collected samples from additional localities to complete the data set and selected samples for more detailed, mineral-scale investigation. The concept behind the sample selection was to cover the temporal distribution of volcanic activity and to choose the freshest rocks, trying to avoid those which show either moderate to pervasive alteration or contain abundant xenocrysts.

The oldest volcanic phase (1220 ka; Panaiotu et al., 2013) is represented by samples from the Racoş volcano and Hegheş scoria cone. We collected samples from the columnar jointed basalt outcrop at the entrance of the Racoş quarry and scoriaceous bombs from the proximal deposit of the nearby Hegheş scoria cone. The younger lava body (800 ka; Panaiotu et al., 2013) of the Bârc quarry is thought to be related to the activity of the La Gruiu scoria cone, which is considered to be the youngest volcano in this area (Seghedi and Szakács, 1994). No Ar–Ar dating is available for these volcanoclastic rocks, but previous K/Ar data indicate a younger age (524 ka; Panaiotu et al., 2004). We collected scoriaceous blocks and bombs from the scoria cone to make a petrologic comparison of the two volcanic products. New Ar–Ar dating (Panaiotu et al., 2013) suggests that the youngest volcanic phase occurred at 680 ka and is represented by basalts from the Mateiaş volcano. We collected fresh basalt samples from the platy-jointed lava breaching the phreatomagmatic unit.

Textural characterization of the mineral phases was performed by combined microscopic and back-scattered electron (BSE) images (prepared by AMRAY 1830 I/T6 SEM at the Department of Petrology and Geochemistry, Eötvös University) followed by determination of their composition using CAMECA SX100 electron microprobe equipped with four WDS and one EDS at the University of Vienna, Department of Lithospheric Research (Austria). The operating conditions were as follows: 15 kV accelerating voltage, 20 nA beam current, 20 s counting time on peak position, focused beam diameter and PAP correction procedure for data reduction. Pyroxenes and oxides were analyzed with a focused 1 μm beam, whereas all feldspar and glass analyses were carried out with an expanded 5 μm beam diameter, minimizing the loss of Na and K. Calibration was based on the following standards: quartz (Si), corundum (Al) albite (Na), olivine (Mg), almandine (Fe), wollastonite (Ca), rutile (Ti), spessartine (Mn), orthoclase (K), Mg-chromite (Cr) and Ni-oxide (Ni).

Major and trace element compositions of the bulk rocks were analyzed at the ACME Labs (Canada; http://www.acmelab.com/). Major and minor elements were determined by ICP-emission spectrometry, whereas trace elements were analyzed by ICP-MS following a lithium borate fusion and dilute acid digestion. Duplicate sample analysis and internal standards were used to check the reliability of the results. One of our samples from Racoş was collected from the same outcrop as that by Downes et al. (1995) and this allows checking the consistency of the two data sets. The major and trace element data of the two samples agree within 10–15% deviation that is well below the analytical error.

4. Petrography and geochemistry

All basaltic samples are olivine-phyric, with 5–20% phenocryst content (Fig. 2). Minor clinopyroxene phenocrysts occur only in the Racoş samples. The groundmass comprises plagioclase, clinopyroxene, olivine, Fe–Ti oxides (mostly Ti-magnetite, ilmenite occurs in the Racoş and Bârc lava) and occasionally volcanic glass. The Racoş and Bârc lavas contain a small amount of nepheline. The scoria samples (Hegheş, Gruiu) are variously vesiculated (up to 40 vol.%) and oxidized (particularly the Hegheş scoriae). In these samples olivines are partially iddingsitized. The olivine phenocrysts (300–1250 μm) are usually euhedral to subhedral, whereas skeletal crystals are found mostly in the Hegheş scoriae. A few olivine

Please cite this article as: Harangi, S., et al., Origin of basaltic magmas of Perşani volcanic field, Romania: A combined whole rock and mineral scale investigation, Lithos (2013), http://dx.doi.org/10.1016/j.lithos.2013.08.025

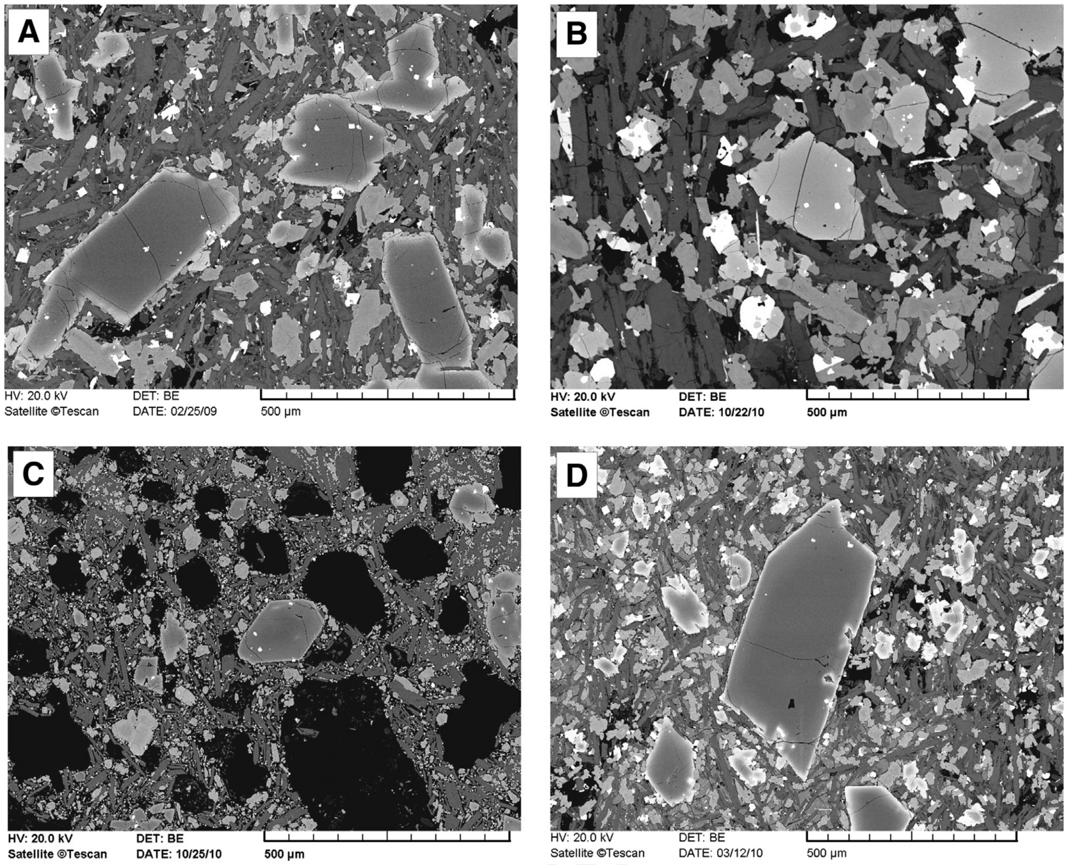

Fig. 2. Textural characterization of the studied samples (BSE images). Note the euhedral to subhedral olivine phenocrysts with spinel inclusions. A. Racoş; B. Mateiaş; C. La Gruiu; D. Bârc.

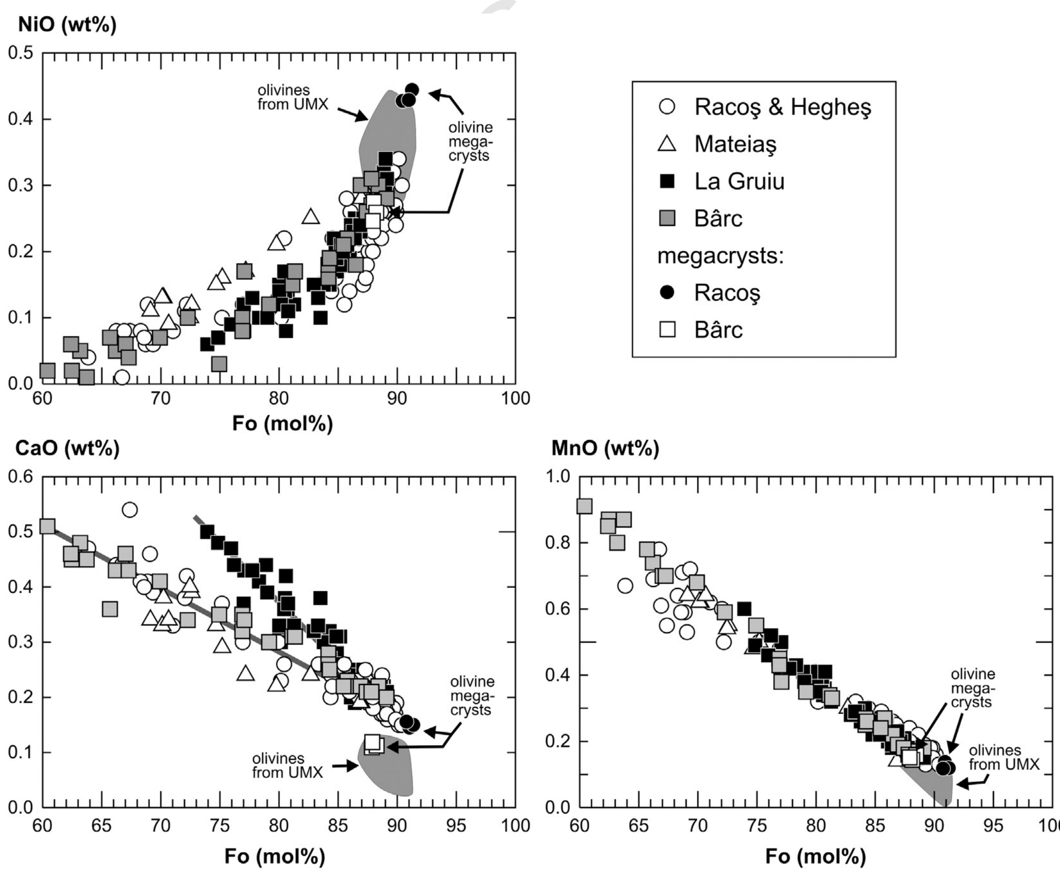

Fig. 3. Compositional variation of olivines. UMX = olivines from ultramafic xenoliths found in the Perşani basalts (Vaselli et al., 1995).

Table 1
Representative compositions of the studied olivine crystals.

	Rac1		Rac2			Barc			GRU-1		gru2		MAT 7a	
	ol1c	ol1r	ol1c	ol1r	ol_gm2	ol7c	ol7r	gm_ol1	ol_6c	ol_6r	ol1 c	ol1 r	ol13 c	ol13 r
SiO_2	40.27	37.02	40.34	40.11	39.89	39.95	36.40	36.23	40.08	38.16	39.97	39.12	39.62	37.33
Cr_2O_3	0.02	0.00	0.03	0.01	0.02	n.a.	n.a.	n.a.	0.02	0.00	0.02	0.02	0.05	0.00
FeO^{tot}	12.17	27.46	9.84	13.33	13.79	13.71	28.59	31.11	13.27	23.46	14.74	17.93	16.03	25.73
MnO	0.21	0.71	0.18	0.25	0.29	0.24	0.70	0.80	0.20	0.60	0.25	0.35	0.30	0.64
NiO	0.24	0.06	0.27	0.14	0.12	0.21	0.06	0.05	0.24	0.06	0.19	0.17	0.25	0.09
MgO	46.80	33.83	48.80	45.78	45.70	45.25	32.61	29.95	46.05	37.33	44.41	41.36	42.93	34.76
CaO	0.21	0.40	0.17	0.21	0.26	0.22	0.46	0.48	0.20	0.50	0.27	0.36	0.24	0.34
Total	99.91	99.48	99.63	99.83	100.07	99.59	98.82	98.62	100.07	100.11	99.83	99.30	99.40	98.89
Fo (mol%)	87.27	68.71	89.84	85.96	85.52	85.47	67.02	63.18	86.08	73.93	84.30	80.44	82.68	70.66

FeO^{tot} = total amount of iron; ol = olivine; n.a. = not analyzed; Rac1 = Hegheş scoria sample; Rac2 = Racoş lava rock sample; Barc = Bârc lava rock sample; GRU-1 = Gruiu lava rock sample; Gru2 = Gruiu scoria sample; MAT 7a = Mateiaş lava rock sample; ol = olivine; c = olivine core; r = olivine rim; gm = groundmass olivine.

megacrysts (defined here as larger than 2000 μm that well exceeds the usual phenocryst size) were observed in the Racoş and Bârc lavas. The phenocrystic olivines have usually homogeneous composition, diffuse normal zoning can be observed only at the outermost margins. Spinel inclusions in olivines are common in all samples. The spinels are 5 to 30 μm in size, vary from euhedral octahedra to anhedral grains, and occur both in the core and the margin of the olivine crystals. They have homogeneous compositions as checked by high magnification BSE images.

The olivine phenocrysts have dominantly 84–90 mol% forsterite content with CaO concentration exceeding 0.15 wt.% (Fig. 3; Table 1). They are compositionally clearly different from the olivines found in ultramafic xenoliths (Vaselli et al., 1995). Less magnesian compositions were measured only at the outer few tens of micron rim of the olivine phenocrysts, mostly in lava samples, whereas olivines in the scoriae have a more restricted Fo-rich (Fo = 87–90 mol%) composition. The Fo component of the margins of the olivines decreases to 60 mol%, however, keeping a linear trend with CaO and MnO contents. Olivines from the youngest scoria cone (La Gruiu) form a slightly different trend in the Fo vs. CaO plot (Fig. 3). In contrast, no difference can be observed in the trends shown by the Fo vs. MnO diagram (Fig. 3). The Ca concentration of the most magnesian olivines (Fo > 84 mol%) is relatively low (<2000 ppm), consistent with the low CaO and FeO contents of the host rocks (CaO = 9–10 wt.%; $Fe_2O_3^{tot}$ = 9–10 wt.%).

Clinopyroxene phenocrysts are found only in the Racoş and Bârc samples, where they have similar compositions (Table 2). They are ferroan-diopside with Mg-number (Mg^{2+} / (Mg^{2+} + Fe^{2+})) ranging from 0.87 to 0.92, with Cr_2O_3 content of 0.15–0.55 wt.%. The Al_2O_3 concentration varies between 3.5 and 8.5 wt.%. The Ti/Al ratio is between 0.125 and 0.25 (Fig. 4).

Spinel inclusions in olivine phenocrysts are chromian spinels (Cr_2O_3 = 18–35 wt.%, Al_2O_3 = 23–40 wt.%). Most have TiO_2 content ranging from 0.5 to 1.0 wt.%, suggesting that they are magmatic spinels and formed from less differentiated magma. Spinels from the Mateiaş basalt show, however, distinct compositional features, such as slightly higher TiO_2 (0.9–1.2 wt.%) and significantly lower Mg-number (0.3–0.4, whereas the spinels from the other samples are between 0.5 and 0.7) consistent with derivation from more evolved magma (Roeder et al., 2003). This is also supported by their relatively higher Fe^{3+} content (Fig. 5) and the lower Fo component (<80 mol%) of their host olivines. The less differentiated spinels form two compositional groups, a Cr-rich group with Cr-number (Cr^{3+} / (Cr^{3+} + Al^{3+})) of 0.38–0.45 (Cr_2O_3 = 28–35 wt.%) and a Cr-poor group with Cr-number of 0.23–0.32 (Cr_2O_3 = 18–23 wt.%; Table 3.). Remarkably, they represent the older (Cr-rich spinels in Racoş and Hegheş) and the younger (Cr-poor spinels in Bârc and La Gruiu) basalt groups, respectively (Fig. 5).

Bulk rock compositions of the studied samples show fairly similar characters (Table 4.). They are all silica-undersaturated (S.I. is between −17 and −8, where S.I. is defined by Fitton et al., 1991) trachybasalts (hawaiite) with relatively high Mg-number (Fe^{2+} is calculated assuming Fe_2O_3/FeO = 0.2) ranging from 0.67 to 0.73. The SiO_2 content is in a narrow range (47–49 wt.%); however, it shows a strong negative correlation with total iron. Concentrations of Ni, Cr and other compatible elements are high, consistent with the high Mg-number of the Perşani basalts. The normalized rare earth element (REE) patterns are light REE-enriched and smooth (Fig. 6). The $(La/Yb)_N$ is in the range of 10–13, which is relatively low compared with other alkali basalts in the Pannonian Basin (Ali and Ntaflos, 2011; Ali et al., 2013; Dobosi et al., 1995; Embey-Isztin et al., 1993; Harangi et al., 1995). The primitive mantle normalized trace element patterns (Fig. 6) are also fairly

Table 2
Representative analyses of the studied chromian spinels.

	Rac1		Rac2		Barc		GRU-1		gru2		MAT 7a	
	sp2_in_ol1	sp1_in_ol6_1	sp_in_ol2	sp1_in_ol7	sp_in_ol5	sp_in_ol10	sp1	sp_6	sp in ol5	sp in ol10	sp in ol3	sp in ol6
SiO_2	0.13	0.08	0.09	0.15	0.22	0.13	0.70	0.24	0.13	0.15	0.08	0.07
TiO_2	0.93	0.72	0.73	0.76	1.02	0.79	1.70	0.96	0.87	0.96	1.17	0.86
Al_2O_3	30.93	26.42	26.92	29.96	34.73	39.73	29.90	39.17	38.50	36.12	23.45	24.07
Cr_2O_3	28.80	35.04	31.49	31.51	20.74	19.39	21.14	19.87	20.32	19.81	21.26	23.01
Fe_2O_3	7.79	5.90	9.89	8.55	8.73	7.63	13.17	7.77	8.24	10.08	18.94	17.33
FeO	16.02	19.50	15.60	9.91	19.83	15.06	18.91	14.78	14.43	16.24	25.48	24.40
MnO	0.15	0.33	0.30	0.38	0.28	0.16	0.27	0.16	0.16	0.26	0.45	0.41
MgO	13.78	10.87	13.33	17.48	11.40	15.10	12.47	15.47	15.45	13.85	6.34	6.96
NiO	0.18	0.12	0.17	0.13	0.14	0.22	0.15	0.26	0.19	0.15	0.09	0.10
Total	98.71	98.97	98.52	98.84	97.07	98.20	98.41	98.66	98.29	97.61	97.25	97.20
Mg#	0.61	0.50	0.60	0.76	0.51	0.64	0.54	0.65	0.66	0.60	0.31	0.34
$Fe^{2+}/(Fe^{2+} + Mg)$	0.39	0.50	0.40	0.24	0.49	0.36	0.46	0.35	0.34	0.40	0.69	0.66
Cr#	38.45	47.08	43.97	41.37	28.61	24.67	32.17	25.39	26.15	26.90	37.81	39.08

Fe_2O_3 is calculated on the basis of stoichiometry; Mg# = Mg / (Mg + Fe^{2+}); Cr# = 100 ∗ Cr / (Cr + Al); sp = spinel; ol = olivine; Rac1 = Hegheş scoria sample; Rac2 = Racoş lava rock sample; Barc = Bârc lava rock sample; GRU-1 = Gruiu lava rock sample; Gru2 = Gruiu scoria sample; MAT 7a = Mateiaş lava rock sample.

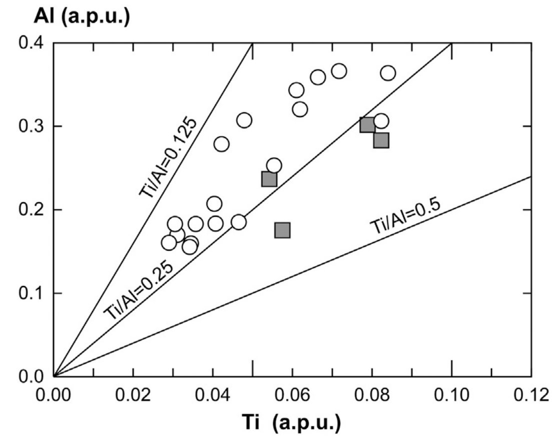

Fig. 4. Al vs. Ti diagram for the clinopyroxene microphenocrysts. The Ti/Al ratio suggests crystallization at relatively high-pressure.

Table 3
Representative compositions of the studied clinopyroxenes.

	Rac1		Rac2		Barc		GRU-1	
	cpx4c	cpx4r	cpx_fen1c	cpx_gm2	cpx_gm2	cpx_gm2	cpx_3c	cpx_3r
SiO_2	47.23	45.63	50.30	48.42	46.32	48.07	46.45	45.42
TiO_2	1.72	2.92	1.12	1.52	2.80	1.92	2.21	2.83
Al_2O_3	7.05	6.92	3.91	6.41	6.82	5.37	7.95	7.88
Cr_2O_3	0.30	0.00	0.15	0.34	0.02	0.44	0.62	0.00
Fe_2O_3	4.54	5.03	2.55	2.84	3.65	2.33	4.13	4.38
FeO	2.11	4.00	3.45	3.30	4.48	4.21	2.44	4.14
MnO	0.12	0.14	0.15	0.13	0.15	0.16	0.13	0.19
MgO	13.62	12.22	15.63	14.09	12.24	14.13	13.12	11.71
CaO	23.05	22.44	22.30	22.82	22.64	22.06	22.80	22.61
Na_2O	0.42	0.54	0.24	0.32	0.53	0.30	0.50	0.57
Total	100.14	99.85	99.81	100.19	99.64	98.99	100.36	99.73
Mg#	0.80	0.72	0.83	0.81	0.74	0.80	0.79	0.72
En	40.37	36.78	44.69	41.62	37.15	42.03	39.72	35.91
Wo	49.13	48.56	45.84	48.45	49.39	47.18	49.60	49.85
Fs	10.50	14.65	9.47	9.93	13.47	10.79	10.68	14.24

Fe_2O_3 is calculated on the basis of stoichiometry; Mg# = Mg / (Mg + Fetot); cpx = clinopyroxene microphenocryst; cpx_fen = clinopyroxene phenocryst; cpx_gm = groundmass clinopyroxene; Rac1 = Hegheş scoria sample; Rac2 = Racoş lava rock sample; Barc = Bârc lava rock sample; GRU-1 = Gruiu lava rock sample.

similar. They show features of the Group 2 basalts in the Pannonian Basin as defined by Harangi and Lenkey (2007), i.e. they are less enriched in the incompatible trace elements than the Group 1 basalts and do not have a negative K-anomaly. The youngest Mateiaş basalt differs from the other samples in having a slightly higher trace element content. Overall, the trace element patterns of the Perşani basalts are typical of the intraplate alkaline basalts worldwide.

5. Discussion

The Perşani basalts were formed by intermittent eruptions in a time span from 1.2 Ma to 600–700 ka, according to new $^{40}Ar/^{39}Ar$ dating (Panaiotu et al., 2013). In order to constrain the origin of the magmas, it is necessary to consider the following observations. The volcanism occurred in a restricted area (ca. 180 km^2) and certainly had a tectonic control. Volcanic eruptions produced low-volume basaltic lavas and pyroclastic rocks. The volcanic activity took place partly coevally with high-K calc-alkalic magmatism in the southern Harghita (Seghedi et al., 2011). The Perşani volcanic field is located 40 km from the Ciomadul volcano, the youngest one (the last eruptions occurred at about 30 ka; Harangi et al., 2010) in the area and about 100 km from the seismically active Vrancea zone, where a deep vertical slab is inferred. Recent geophysical studies indicate the presence of a low-velocity anomaly at lower crustal levels both beneath the Perşani area and the Ciomadul volcano (Popa et al., 2012), while deep seismic models imply a low-velocity anomaly in the upper mantle down to 110 km (Martin et al., 2006) or to 400 km (Ren et al., 2012). Ultramafic and mafic xenoliths occur frequently in the volcanic products (Vaselli et al., 1995). In the next section, we will discuss the origin of the magmas in the following structure: first the role of possible crustal contamination and crystal fractionation is evaluated, followed by constraining the conditions of melt generation (degree of melting, melting pressure and temperature). This is followed by characterization of the mantle sources and how these changed with time. The magma ascent rate is estimated based on the Ca-profile in xenocrystic olivine and finally, all the information is integrated to imply the geodynamic situation.

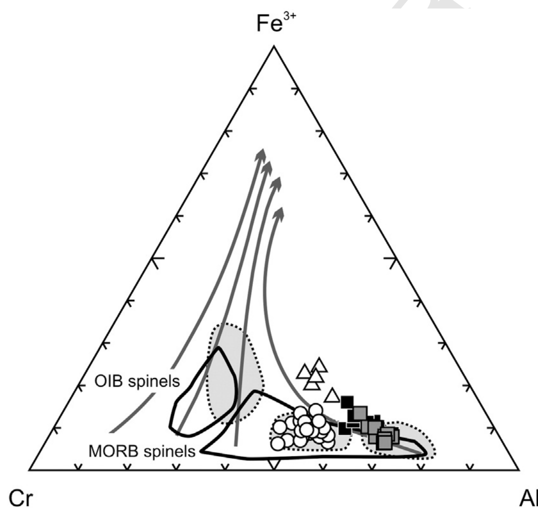

Fig. 5. Compositional characteristics of spinels inclusions in olivine phenocrysts based on the Cr–Fe^{3+}–Al diagram. The Perşani spinels form two compositionally coherent groups and fall into the MORB spinel field as defined by Roeder et al. (2001). OIB spinel field is denoted based on the composition of the spinels from Hawaii after Roeder et al. (2003). The arrows show fractionation trends of spinels. The three gray fields defined by the spinel composition data from several alkaline basalt localities from the Carpathian–Pannonian region (Harangi, 2012; Jankovics et al., 2012, 2013). Symbols are explained in Fig. 3.

5.1. The role of fractional crystallization

The Perşani basalts have relatively high Mg-number (0.67–0.73), high Ni (150–220 ppm) and Cr (250–500 ppm) contents, indicating near-primary compositions and therefore showing only minimal crystal fractionation. They often contain abundant mantle xenoliths and these features all imply a fast magma ascent. Trace element ratios such as Nb/Th (5–10) and Nb/La (1–1.5) are typical of mantle-derived melts and higher than the continental crust (Rudnick and Fountain, 1995). Thus, we can conclude that crustal contamination did not significantly modify the magma composition.

In general, olivine and spinel are liquidus phases during crystallization of alkaline silica-undersaturated mafic magmas (Roeder et al., 2006), although as Smith et al. (2008) pointed out, early-stage crystallization of clinopyroxene should be also considered even if it cannot be observed as a phenocryst. Early crystallization of clinopyroxene modifies not only the melt composition, but can also influence the composition of co-existing evolving phases, such as olivine and spinel. In the Perşani basalts olivine is the principal phenocryst phase and commonly contains spinel inclusions. Clinopyroxenes occur only in the microphenocryst assemblage. This can usually be interpreted that olivine and spinel crystallized first as liquidus phases, followed by formation of minor clinopyroxene

Table 4
Bulk rock compositions of the alkaline basalts from Perşani Mts.

	Rac 1	Barc	Gru 1	Gru 2	Mat
SiO_2	46.87	46.63	46.68	46.08	46.72
TiO_2	1.55	1.77	1.78	1.75	1.73
Al_2O_3	15.8	15.95	16.02	16.07	15.61
Cr_2O_3	0.06	0.05	0.04	0.04	0.06
Fe_2O_3	9.57	10.12	9.55	9.86	9.69
MnO	0.16	0.17	0.16	0.17	0.16
MgO	9.68	9.22	8.64	8.82	9.66
CaO	9.85	9.44	9.35	9.28	9.41
Na_2O	3.79	3.91	3.24	3.46	4.05
K_2O	1.63	1.91	1.93	2.02	2.03
NiO	0.03	0.02	0.2	0.2	0.03
P_2O_5	0.39	0.48	0.5	0.52	0.56
LOI	0.2	0	1.7	1.5	0
Total	99.58	99.67	99.79	99.77	99.71
mg#	69	66.7	66.6	66.3	68.7
Ce	60.9	63.9	59.3	60.7	102
Pr	6.96	7.59	6.85	7.03	n.a.
Nd	28.2	34	27.8	28.8	39
Sm	5.18	6.04	5.12	5.22	n.a.
Eu	1.58	1.86	1.66	1.75	n.a.
Gd	4.26	5.14	4.79	4.98	n.a.
Tb	0.6	0.7	0.74	0.76	n.a.
Dy	3.91	4.35	3.98	4.08	n.a.
Ho	0.75	0.83	0.77	0.76	n.a.
Er	2.05	2.26	2.16	2.16	n.a.
Tm	0.29	0.34	0.29	0.29	n.a.
Yb	1.97	2.21	1.75	1.83	n.a.
Lu	0.28	0.31	0.28	0.28	n.a.
TOT/C	<0.02	<0.02	<0.02	<0.02	n.a.
Pb	2.2	3.6	8.1	5.2	8.3
Ni	172.8	153.6	154	169	n.a.
Mo	3.7	3.7	2.8	2.9	n.a.
Cu	36	44	38.6	34	54
Zn	38	60	75	72	77
TOT/S	<0.02	<0.02	<0.02	<0.02	n.a.
As	0.5	0.7	2.1	2.3	n.a.
Cd	<0.1	<0.1	<0.1	0.1	n.a.
Sb	<0.1	<0.1	<0.1	<0.1	n.a.
Bi	<0.1	<0.1	<0.1	<0.1	n.a.
Ag	<0.1	<0.1	<0.1	<0.1	n.a.
Au	<0.5	<0.5	1.1	<0.5	n.a.
Hg	<0.01	<0.01	<0.01	<0.01	n.a.
Tl	<0.1	<0.1	<0.1	<0.1	n.a.
Se	<0.5	<0.5	<0.5	<0.5	n.a.
Sc	27	26	23	23	22
Ba	685	758	735	726	1013
Be	2	2	1	1	n.a.
Co	44.1	41.1	38	39.8	n.a.
Cs	1	1	0.8	0.9	n.a.
Ga	17.9	17.9	18.2	17.2	n.a.
Hf	3.7	4.5	4.2	4.4	4.4
Nb	37.6	51.8	47.3	48.8	52.6
Rb	37.9	43.1	39.4	39.5	51.5
Sn	1	2	1	2	n.a.
Sr	813.6	775	771	820.4	863
Ta	2.4	3.1	2.9	2.9	3.79
Th	5.6	6	5	5.5	9.4
U	1.7	1.7	1.2	1.5	n.a.
V	199	194	188	195	206
W	0.8	0.8	0.6	0.7	n.a.
Zr	154.8	185.3	174.3	181	209
Y	21.6	23.8	20.8	22	23.5
La	32.3	32.8	31.9	31.7	53

Major elements are in wt.%; minor and trace elements are in ppm; Mg# = Mg / (Mg + Fe^{2+}), where Mg and Fe^{2+} are cation fractions; LOI = loss of ignition; n.a. = not analyzed; Rac1 = Hegheş scoria sample; Barc = Bârc lava rock sample; Gru 1 = Gruiu lava rock sample; Gru2 = Gruiu scoria sample; Mat = Mateiaş lava rock sample from Downes et al. (1995) paper.

en route to the surface. Nevertheless, the Ca deficiency (Herzberg, 2011; Herzberg and Asimow, 2008) in the olivines and the bulk rocks might indicate that high-pressure clinopyroxene crystallization could have also occurred.

Using the mathematical formulation proposed by Smith et al. (2008), the minimum pressure of clinopyroxene fractionation can be estimated. We got pressure values of 1.3–1.6 GPa, which correspond to depths of 45–55 km. In contrast, the clinopyroxene–liquid thermobarometer of Putirka et al. (1996) yields a significantly lower pressure (0.8–1.2 GPa) for clinopyroxene crystallization at a temperature of about 1250 °C. For the most magnesian olivines, however, we got a higher crystallization temperature (1300–1350 °C) using the olivine–liquid FeO/MgO distribution (Roeder and Emslie (1970), the olivine–liquid CaO/MgO relationship (Jurewicz and Watson, 1988) and the calculation scheme provided by Putirka et al. (2007) and Putirka (2008). In this calculation the bulk rock compositions were used as liquid compositions and from each sample the most magnesian olivines (crystal cores) were chosen. The selected olivine–liquid composition pairs fulfill the equilibrium criteria based on the Rhodes diagram (Rhodes et al., 1979). In conclusion, the estimated crystallization temperatures suggest that olivine crystallization occurred prior to formation of clinopyroxenes. The lack of early-stage clinopyroxene crystallization is inferred also from other observations. The Sc content, which is sensitive to clinopyroxene fractionation, is high in the Perşani basalts (Sc = 22–28 ppm), the highest among the basalts in the Pannonian basin. Furthermore, the Cr-number of spinels is constant along with various Fo content of coexisting olivines that can be explained by crystallization of only olivine and spinel during the early stage of the magma evolution (Arai, 1994; Smith and Leeman, 2005). Thus, high pressure clinopyroxene crystallization could not be responsible for the relatively low Ca content of the Perşani olivines and bulk rocks.

The crystallization history of the Perşani mafic magmas can be summarized as follows. Magnesian olivines crystallized along with spinels as liquidus phases at 1300–1350 °C, presumably in the upper mantle. The primitive character of the spinel inclusions in olivine is indicated also by their low Ti and Fe^{3+} content. This is similar to spinels in the Cascades basalts (Smith and Leeman, 2005), but is in contrast to the more evolved spinel compositions found in the basalts of Paricutin (Bannister et al., 1998) and southwest Japan (Shukuno and Arai, 1999). The rapidly increasing Ca content of the olivines with decreasing Fo content suggests polybaric compositional evolution (Stormer, 1973). Olivine and spinel fractionation was followed by crystallization of clinopyroxene that took place at about 1250 °C temperature and at deep crustal levels (at 0.8–1.2 GPa; i.e. 25–40 km depth), consistent with their Ti/Al ratio (0.125–0.25; Fig. 4) and Al^{VI}/Al^{IV} ratios (>0.25). The low-pressure mineral assemblage (plagioclase, Fe–Ti oxides, nepheline) was formed at or near the surface.

5.2. Conditions of magma generation

The composition of the erupted magma as well as some key minerals such as olivine and spinels depends upon the conditions of magma generation (Herzberg, 2011; Kamenetsky et al., 2001; Niu et al., 2011; Roeder et al., 2001; Sobolev et al., 2007). The Perşani basalts with their near-primitive bulk composition, along with the compositional features of the liquidus minerals (olivine and spinel), provide an excellent opportunity to have a deep insight into this process and constrain the temperature, pressure (depth) and degree of melting. Reconstruction of these parameters has an important inference on the geodynamic environment of the basaltic volcanism.

Alkaline silica-undersaturated mafic magmas can be generated by low-degree of melting either in the upwelling asthenosphere (Bradshaw et al., 1993; Niu et al., 2011; Wang et al., 2002) or by melting of metasomatic, usually amphibole-rich, veins in the lithosphere (Beccaluva et al., 2007; Bianchini et al., 2008; Fitton et al., 1988; Pilet et al., 2008; Valentine and Perry, 2007). In the first case, upward movement of mantle rock is required (decompressional melting), whereas in the second case either significant thinning of the lithosphere or a thermal perturbation is necessary. Delamination and recycling of the metasomatized lithosphere into the convecting

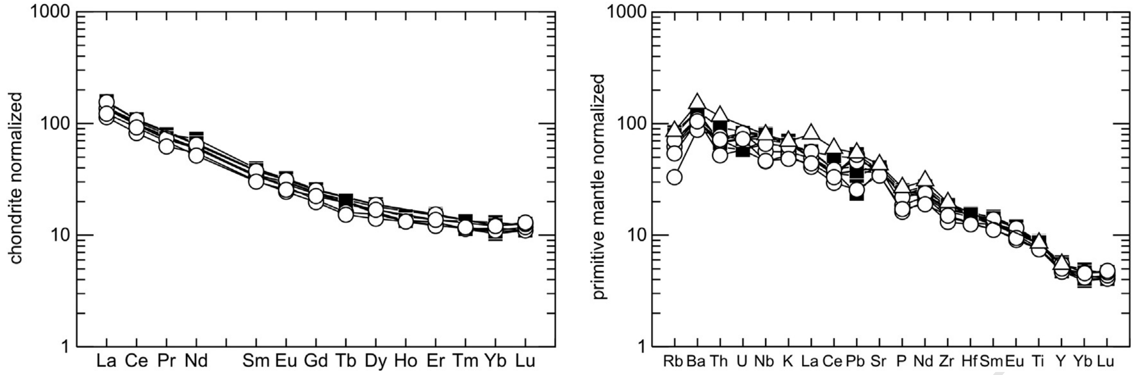

Fig. 6. Chondrite normalized rare-earth element and primitive mantle normalized trace element patterns of the Perşani basalts. Symbols are explained in Fig. 3. Data for normalization are from McDonough and Sun (1995).

mantle could be another scenario to produce alkaline mafic magma (Lustrino, 2005). Amphibole megacrysts are occasionally found in the Perşani basalts and they have similar Sr–Nd isotopic composition as the host rocks (Downes et al., 1995). This suggests a genetic relationship and could be consistent with the metasomatized lithospheric origin of the Perşani mafic magmas.

Constraining the mineralogical assemblage of the mantle source of the Perşani magmas using trace element modeling, it is possible to test whether amphibole had a role in melt generation. Trace element ratios of Zr/Nb and La/Y were chosen, because their values are not dependant on early-stage crystal fractionation and are sensitive on the presence of spinel, garnet and amphibole in the mantle source. The result of the model calculations is shown in Fig. 7, along with the data of the Perşani basalts. Residual garnet in the source primarily influences the La/Y ratio of the generated magma, whereas amphibole mostly controls the Zr/Nb ratio. The Perşani basalts plot between the garnet- and spinel-lherzolite model lines and do not fit with the model of melting of amphibole-bearing lithology. Another argument against the presence of amphibole in the source is the lack of any correlation between K and other incompatible trace elements. The primitive mantle normalized trace element patterns (Fig. 6) do not show a negative K-anomaly, which could indicate a residual K-bearing phase during mantle melting. Total consumption of amphibole can account for this feature, but in this case it would require a more potassic composition along with enrichment in other elements. Furthermore, the composition of spinels in the Perşani basalts differs from that of spinels found in the ultramafic xenoliths (Vaselli et al., 1995; Szabó Á., unpublished MSc thesis, 2013) and therefore implies a source region different from the lithospheric mantle beneath Perşani. The trace element modeling is consistent with magma generation in the presence of both garnet and spinel. Klemme (2004) conducted high pressure and high temperature experiments and showed that coexistence of garnet and spinel in mantle peridotite could be in a larger depth range in the case of a Cr-bearing system. In summary, we can infer that the alkaline basaltic magmas which fed the Perşani volcanism could have been formed in the sublithospheric mantle in the spinel-garnet stability field. In the next paragraphs we attempt to constrain the pressure and temperature conditions of melting.

Formation of the primary basaltic magmas during decompression of upwelling mantle material occurs in a depth range controlled by the

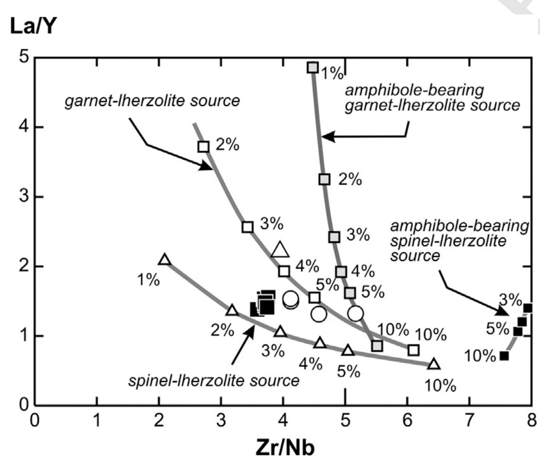

Fig. 7. Trace element modeling for the melt generation beneath the Perşani area. Model parameters: non-modal equilibrium partial melting process with the following source rocks: spinel-lherzolite–olivine (57%), orthopyroxene (25.5%), clinopyroxene (15%), spinel (2.5%); garnet-lherzolite–olivine (60.1%), orthopyroxene (18.9%), clinopyroxene (13.7%), garnet (7.3%); amphibole-bearing spinel-lherzolite–olivine (56%), orthopyroxene (22%), clinopyroxene (10%), spinel (2%), amphibole (10%); amphibole-bearing garnet-lherzolite–olivine (60.1%), orthopyroxene (18.9%), clinopyroxene (11%), garnet (6%) and amphibole (4%). Melting modes: $ol_{1.21}opx_{8.06}cpx_{76.37}sp_{14.36}$, $ol_{1.3}opx_{8.7}cpx_{36}gt_{54}$, $ol_{1}opx_{8}cpx_{30}sp_{10}am_{51}$, $ol_{1}opx_{1}cpx_{15}gt_{25}am_{58}$, respectively. Source rock composition: La and Nb — 4 × primitive mantle values (2.59 and 2.63 ppm, respectively), Zr — 2 × primitive mantle values (21 ppm) and Y — 1.5 × primitive mantle values (6.45 ppm). Symbols are explained in Fig. 3.
Distribution coefficients are from Kostopoulos and James (1992), while for amphiboles from McKenzie and O'Nions (1991).

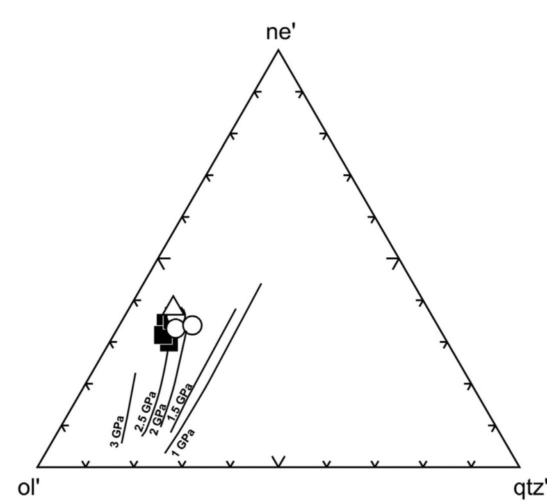

Fig. 8. Determination of melting pressure based on the calculated primary magma compositions of the Perşani basalts using the ol′–ne′–qtz′ plot of Hirose and Kushiro (1993). ol′ = ol + 0.75opx; ne′ = ne + 0.6ab; qtz′ = qtz + 0.4ab + 0.25opx, where ol, opx, ne, ab and qtz are CIPW normative mineral components. Symbols are explained in Fig. 3. Melting pressure lines are after Sakuyama et al. (2009).

Please cite this article as: Harangi, S., et al., Origin of basaltic magmas of Perşani volcanic field, Romania: A combined whole rock and mineral scale investigation, Lithos (2013), http://dx.doi.org/10.1016/j.lithos.2013.08.025

mantle solidus and the mantle potential temperature (initial melting depth) and the thickness of the lithosphere (final melting depth; Langmuir et al., 1992; Niu et al., 2011). In the estimation of melting depth and temperature, first the primary magma compositions have to be calculated correcting for even the minor amount of fractional crystallization. For this, an appropriate amount of olivine was added to the bulk rock data using the method of Herzberg and Asimow (2008). An acceptable result was achieved after correction of 5–12% olivine crystallization. The modeled primary magma composition depends, however, also on the estimation of the Fe_2O_3 content of the magma. Conventional analytical techniques give the total iron as total Fe_2O_3 and an assumption is necessary to divide this into FeO and Fe_2O_3. Herzberg and Asimow (2008) suggested that Fe^{2+}/Fe^{tot} around 0.9 could give a reliable result, however, many ocean island basalts (OIB) are more oxidized and an adjustment based on the relative amount of Fe_2O_3 and TiO_2 could yield more appropriate data. Fixing the Fe_2O_3/TiO_2 ratio to 1, less olivine correction (1–7%) is necessary to achieve the primary magma composition of the Perşani basalts. However, increasing the Fe_2O_3 value leads to a decrease of the MgO content of the primary magma and as a consequence a decrease of the mantle potential temperature (by about 50 °C) and minor increase of melt fractions. In contrast, it does not significantly affect the melting pressure estimate.

The initial and final melting pressures were calculated using different techniques. Experiments conducted by Takahashi and Kushiro (1983) and Hirose and Kushiro (1993) on anhydrous peridotite show that the most pressure-sensitive major oxides are SiO_2 and FeO, whereas CaO and Al_2O_3 depend mainly on the degree of partial melting and the composition of the source rock. Scarrow and Cox (1995) formulated this relationship, providing a simple equation for the apparent pressure of melt segregation. Wang et al. (2002) revised this equation using a more extended experimental data set and got a third-order polynomial fit between SiO_2 and the melting pressure. This equation yields a slightly higher pressure than that of Scarrow and Cox (1995). For the Perşani primary magma composition, we got 2.2–2.7 GPa pressure using the equation of Wang et al. (2002). This corresponds to a depth of 75–90 km (calculated based on 40 km crust with 2.85 g/cm^3 and an underlying mantle with 3.25 g/cm^3 average density values). A similar pressure range (1.9–2.6 GPa) was obtained using the ol′–ne′–qtz′ normative diagram (Fig. 8) of Hirose and Kushiro (1993). The melting pressure lines in this plot were refined by an extended experimental data set by Sakuyama et al. (2009).

Langmuir et al. (1992) used experimental data and numerical model to constrain the depth and extent of mantle melting for mid-ocean ridge basalts. This is based on the FeO and Na_2O content of the primary magmas, as FeO indicates the depth of melting, whereas Na_2O is sensitive to the degree of melting. Wang et al. (2002) extended this technique to continental basalts and outlined a mantle melting profile across the Basin and Range, SW USA. The FeO content does not change significantly during crystal fractionation in high MgO (>8 wt.%) basalts and its total value depends on the pressure and temperature of initial melting. Thus the total FeO content of the calculated primary magma composition can be used to infer the initial melting pressure. During adiabatic upwelling of the mantle, the extent of melting increases until magma generation ceases, i.e. at the final pressure. During this process, FeO does not change greatly (up to about 0.5 wt.%), whereas Na_2O decreases significantly. We adopted the methodology described in Langmuir et al. (1992) and Wang et al. (2002) and got 2.0–2.5 GPa initial melting pressure that drops to 1.8–2.0 GPa during decompression melting. This corresponds to a melting column between 61–68 km and 68–83 km.

To further constrain the melting conditions of the Perşani basalts, we also used the geothermobarometric calculation provided by Lee et al. (2009). This formulation requires peridotite melting. The obtained pressure values (1.8–2.5 GPa) are consistent with the above results, whereas we got 1350–1420 °C for the melting temperature. This temperature range fits perfectly that provided by the PRIMELT2 software of Herzberg and Asimow (2008; T_p = 1380–1420 °C using Fe^{2+}/Fe^{tot} around 0.9 for calculation the primary magma composition). This calculated mantle potential temperature is the lowest obtained for alkaline basalts of the Pannonian Basin. This result implies melting at normal mantle potential temperature beneath Perşani. Thus, melting of the lower lithosphere beneath this area does not seem to be feasible, since there is no indication of a thermal anomaly necessary for this and composition of the basalts does not show derivation from a metasomatized mantle source, which is capable of melting without decompression. Melting could have occurred in the upwelling asthenosphere and, considering the obtained melting pressure range, this place the lithosphere–asthenosphere boundary not deeper than 60 km. This is consistent with the geophysical result of Martin et al. (2006) and is in contrast to the thick lithosphere interpretations (Dérerova et al., 2006; Horváth et al., 2006).

5.3. Mantle source characteristics

In the previous section, we concluded that the Perşani magmas originated at 60–85 km by decompressional partial melting of upwelling asthenospheric mantle material. The pressure, temperature and degree of melting closely influenced the composition of the primary melt; however, another important controlling factor is mantle compositional variation. This influences not only the bulk magma composition, but also

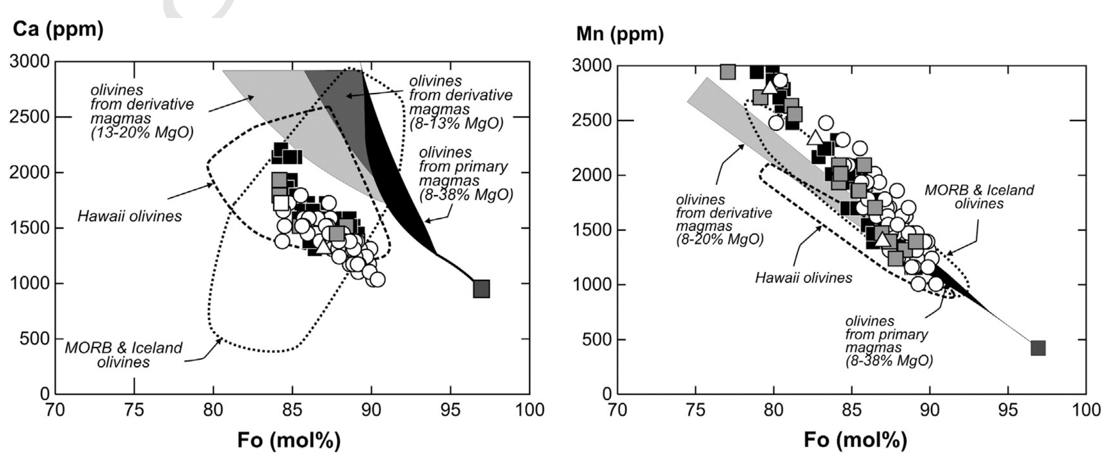

Fig. 9. Comparison of the composition of the Perşani olivines with literature data and the Herzberg (2011) modeling result. Symbols are explained in Fig. 3. MORB, Iceland and Hawaii olivine fields are after Sobolev et al. (2007).

Please cite this article as: Harangi, S., et al., Origin of basaltic magmas of Perşani volcanic field, Romania: A combined whole rock and mineral scale investigation, Lithos (2013), http://dx.doi.org/10.1016/j.lithos.2013.08.025

provides a fingerprint in the mineral chemical data. Olivine and spinel compositions are particularly sensitive to mantle source features.

The Perşani basalts and their olivine phenocrysts are characterized by relatively low Ca (Fig. 9A). Herzberg and Asimow (2008) and Herzberg (2011) suggested that this feature implies that pyroxenite could also have been present in the mantle source region, assuming that no high-pressure clinopyroxene fractionation occurred. Although we excluded that early stage clinopyroxene crystallization depleted the Ca content of the Perşani magma and, as a result, caused low Ca also in the olivine phenocrysts, this feature cannot be explained even by pyroxenite melting. The olivines in the Perşani basalts have relatively low Ni and high Mn (Fig. 9B; resulting in low Fe/Mn ratio) concentrations that is just the opposite of what was required in the case of pyroxenite melting (Sobolev et al., 2007). In fact, the geochemical features of the Perşani olivines resemble the olivines from MORB and from Iceland basalts and this implies peridotitic source of the magmas. Furthermore, Niu et al. (2011) questioned whether the "pyroxenite-signature" proposed by Sobolev et al. (2007) exists at all and suggested that this can be equally explained by the lid-effect, i.e. by variations in lithospheric thickness. Magmas generated under a thin lithosphere could crystallize olivines with relatively low Ni and high Mn and corresponding low Ni/Mg, low Ni/(Mg/Fe) and high Mn/Fe and high Ca/Fe ratios. All of these features characterize the Perşani olivines except for the high Ca/Fe ratio (in fact, they have low Ca and therefore a low Ca/Fe ratio). This interpretation, i.e. melt generation under a thin lithosphere is consistent with the geobarometric results described above. Thus, the Perşani magmas could have originated dominantly from a peridotitic mantle source, although it is still unresolved what caused the Ca deficiency in the host rock and in the most magnesian olivines.

A further constraint on the mantle source characteristics can be given using the compositions of spinel inclusions in magnesian olivine phenocrysts, which are ubiquitous in the Perşani basalts. Composition of spinels carries important petrogenetic information as pointed out by many authors (Arai, 1994; Dick and Bullen, 1984; Kamenetsky et al., 2001; Roeder et al., 2003; Smith and Leeman, 2005). As discussed above, the low Ti and Fe^{3+} content of spinels in the Perşani olivines implies that they could have been formed during the early stage of magma evolution. These spinels are enclosed by olivines with Fo content ranging from 84 to 89 mol%. In contrast to this limited compositional variation of olivines, the Mg-number of the spinels shows a relatively large range from 0.32 to 0.78. The Mg-number of the spinels depends, however, not only on the composition of the melt, but also on the substitution of other elements (Fe–Cr for Mg–Al) and on possible re-equilibration at lower temperature (Kamenetsky et al., 2001). Kamenetsky et al. (2001) showed that subaerial lavas contain spinel inclusions with relatively lower Mg-number (by up to 10 mol%) due to the slower cooling rate compared with spinels in quenched MORBs. Thus, the relatively large variation in the Mg-number of the Perşani spinels could be explained by the cooling rate effect (in fact, our samples represent both lavas and scoria).

In contrast to the Mg and Fe, the abundances of Al, Cr and Ti in spinel vary much less during post-entrapment re-equilibration and preserve the original character (Kamenetsky et al., 2001). The Cr-number of spinel is a useful indicator of the degree of depletion of the mantle source (Dick and Bullen, 1984) and this fingerprint is preserved even in spinels crystallized from mafic magmas (Arai, 1994). The Cr-number of the Perşani spinels is in the range from 0.23 to 0.45, however, two distinct groups can be recognized (Figs. 5 and 10). These two groups correspond with the samples of the older (Racoş) and younger (Bârc, Gruiu) eruptive phases, respectively. Basalts formed during the first volcanic phase have spinels with higher Cr-number (0.38–0.45) than the younger phase magmas (0.23–0.32). In the spinel Cr-number vs. olivine Fo-content diagram (Fig. 10; Arai, 1994), the two spinel groups form a linear, sub-horizontal array with decreasing olivine Fo-content. Spinel inclusions enclosed by the most magnesian olivines fall just at the edge of the olivine–spinel mantle array and differ from spinels found in the ultramafic xenoliths in Perşani (Vaselli et al., 1995; Szabó Á., unpublished MSc thesis, 2013). The spinel Cr-numbers suggest that the younger phase magmas were generated from a more fertile peridotite source than those of the older phase. Nevertheless, all spinels are relatively Al-rich and resemble those found in MORBs (Fig. 5; Roeder, 1994; Roeder et al., 2001), similar to the MORB-character of the olivine compositions (Fig. 9).

Remarkably, these two coherent groups of Al-rich spinels in the Perşani basalts are recognized also in other basalt occurrences of the Carpathian–Pannonian region (Fig. 10; Harangi, 2012). They were described in spinels found even in single basaltic rocks (Füzes scoria cone; Jankovics et al., 2012). An additional spinel compositional group with even higher Cr-number (0.55–0.65), similar to spinel found in Hawaii (Roeder et al., 2003), are found mostly at the western and northern part of the Pannonian basin. Thus, it appears that the compositional variation of early-stage spinel in alkaline basalts of the Carpathian–Pannonian region suggests three compositionally distinct domains in the sublithospheric upper mantle beneath this region.

In summary, compositional features of the most magnesian olivines and their spinel inclusions in the Perşani basalts are similar to those found in MORB and indicate a slightly depleted mantle source. However, spinel compositions suggest that two distinct mantle domains were involved in magma generation. This can be recognized also in the bulk rock major and trace element data and indicates a change in the mantle source of the basaltic magmas during the evolution of the Perşani volcanic field. Younger basaltic magmas were generated by lower degrees of melting (Fig. 7), from a deeper (Fig. 8) and compositionally slightly different mantle source (Figs. 10 and 13).

5.4. Estimation of the magma ascent rate

Once magma has segregated from the melting column, it starts to ascend due to buoyancy. The primitive nature of the Perşani basalts indicates that the magmas could not have paused too long at any depth in the lithosphere. A fast magma ascent is inferred also from the abundance of ultramafic and mafic xenoliths in some basalts (Vaselli et al., 1995). There is a number of possible ways to calculate the magma ascent rate (a summary is given by Jankovics et al., 2013), here we applied

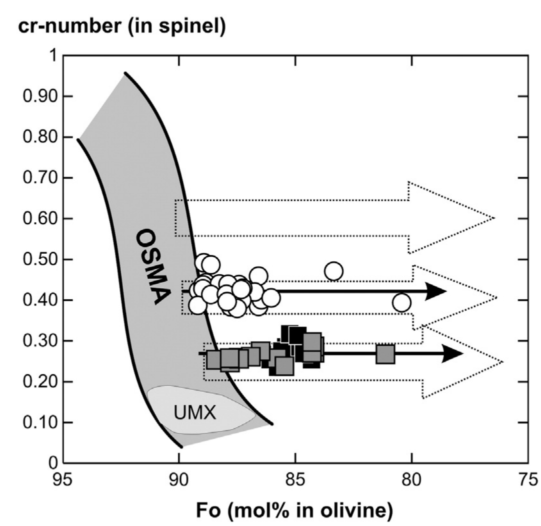

Fig. 10. Spinel Cr-number (Cr / (Cr + Al)) vs. olivine Fo (mol%) content for the coexistent spinel–olivine pairs of the Perşani basalts compared with the olivine–spinel mantle array (OSMA; Arai, 1994) and the spinels found in the ultramafic xenoliths (denoted as UMX) in the Perşani basalts (Vaselli et al., 1995). The subhorizontal trends indicate olivine fractionation, whereas the distinct Cr-numbers of the spinels imply two, slightly different source region of the mafic magmas. The large arrows correspond to the olivine–spinel trends shown by the basalts from the Carpathian–Pannonian region (Harangi, 2012; Jankovics et al., 2012, 2013). Symbols are explained in Fig. 3.

Please cite this article as: Harangi, S., et al., Origin of basaltic magmas of Perşani volcanic field, Romania: A combined whole rock and mineral scale investigation, Lithos (2013), http://dx.doi.org/10.1016/j.lithos.2013.08.025

the time-dependant Ca-diffusion in olivine technique as described by
Q7 Kil and Wendlandt (2004).

Following the incorporation of foreign crystals (either as xenocrysts or crystals in xenoliths) in a melt, complex reactions take place at the crystal margin. Diffusion of minor and trace elements could modify the chemical profile of the mineral and develop a sharp increase of certain elements at the contact with the melt (Costa et al., 2008). In olivines, Ca has a diffusion coefficient that allows a relatively rapid change in the Ca concentration at the outermost rim of the enclosed crystals during relatively short time. The elevated Ca content at the rim of xenocrystic magnesian olivines is attributed to the temperature increase in host basaltic melt and their transport to the surface (Köhler and Brey, 1990). Lasaga (1998) formulated an equation based on the one-dimensional model for Ca-diffusion: $T1/2 = (X1/2)^2 / 2D$, where T1/2 is the time necessary to reach half of the equilibration concentration of Ca in olivine at a distance X1/2 from the rim. The diffusion coefficient (D) for Ca in olivine is $3.18 * 10^{-12}$ cm^2/s at 1200 °C and $f(O_2) = 10^{-8}$ bar (Jurewicz and Watson, 1988; Köhler and Brey, 1990).

We have found rare olivine megacrysts (xenocrysts) in the Perşani basalts where the outermost margin shows an abrupt compositional change. They have a homogeneous inner core composition with Fo content of 91 mol% (Racoş) and 88.1 mol% (Bârc), and clearly differ from the composition of the olivine phenocrysts in the rocks. The CaO concentration of the interior is also stable at 0.16 wt.% and 0.12 wt.%, respectively. The high-resolution olivine profiles show two segments of increasing CaO at the outermost margin (Fig. 11). The first one is characterized by a slow increase along about 200 μm length followed by an abrupt change in the last 40 μm of the crystal. This two-stage Ca variation was recognized also in the olivine profiles of the Rio Grande basalts by Kil and Wendlandt (2004) and they interpreted it two Q8
heating stages. For the Perşani olivines, we calculated 1.2–1.3 years (Fig. 11) for the first heating phase that might have occurred when the lower lithosphere experienced an increase of temperature provided by fresh uprising magma. The second heating stage lasted only 4–5 days (Fig. 11) and this could correspond to the time elapsed between incorporation of the olivine grains into hot magma and the eruption, i.e. the transport time from the depth to the surface. This magma ascent rate value is very similar to what Jankovics et al. (2013) obtained for the Bondoró basalts in the central Pannonian Basin and what Mattsson Q9
(2012) calculated for the ascent of melilitic magma in Tanzania. All of these results suggest that mafic magmas can penetrate the continental crust within a short time, i.e. for a few days. From the point of view of natural hazards, this leaves only limited time for recognition and preparation for a volcanic eruption.

5.5. Geodynamic implications

Our main conclusions about the origin of the Perşani magmas are that they are derived from a heterogeneous mantle source (mostly variously depleted peridotitic MORB-source mantle material) at normal mantle potential temperature in a melting column from 83 to 60 km depth. An important point is the localized and low-volume flux nature of the volcanism with eruption centers that were clearly controlled by the local crustal tectonic conditions, i.e. southwest–northeast trending normal faults.

The Perşani volcanic field is located about 100 km from the seismically active Vrancea zone, where a near-vertical descending slab in the mantle causes intermediate depth earthquakes (Wenzel et al., 1999).

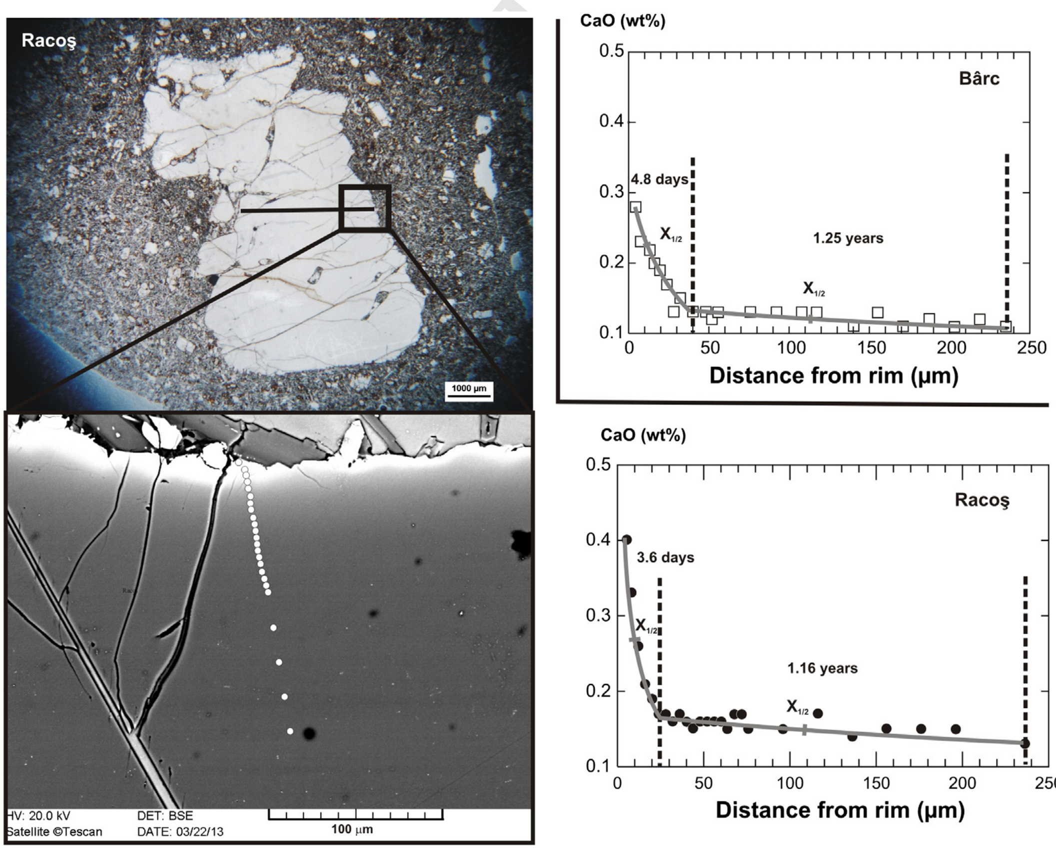

Q3 **Fig. 11.** CaO profile along an olivine xenocryst from the Racoş basalt and the calculation of the duration of heating events based on method of Kil and Wendlandt (2004) for the Racoş and the Bârc samples. Microscopic and BSE images of the olivine megacryst from the Racoş basalt with the profile and the analyzed points shown in the diagram are in the left. Two heating stages can be distinguished: the 1.16–1.25 years could correspond to the heating of the lithospheric mantle by the uprising mafic magma, whereas the 3.6–4.8 days could be the time elapsed while the mafic magma crossed the continental crust, i.e. imply the magma ascent rate.

Although this area is one of the most thoroughly investigated regions of eastern-central Europe, the geodynamic situation is still unclear (Ismail-Zadeh et al., 2012). The conventional explanation is that the final stage of subduction, which started in the Miocene, is going on beneath Vrancea, where the descending slab is just about breaking off (Martin et al., 2006; Sperner et al., 2001; Wortel and Spakman, 2000). Gîrbacea and Frisch (1998) accepting the initial Miocene subduction, but suggested a large scale delamination and roll-back of the detached lower lithosphere from northwest towards Vrancea. Chalot-Prat and Gîrbacea (2000) placed this scenario in the context of the Quaternary volcanism in Perşani and Ciomadul (South Harghita) and suggested upwelling of hot asthenosphere, filling the void left by the delaminated lithospheric material. However, this delamination model requires a relatively large magma production in a more extended area and a temporal southeastward shift of the volcanism, neither of them is observed. Instead a localized and low-flux magma production rate occurred in the Perşani volcanic field. In the seismic tomography model provided by Martin et al. (2006), a low-velocity anomaly in a depth range of 70–110 km can be seen northwestward from the Vrancea zone, just about beneath the Perşani area. Our petrogenetic result (i.e., melting in 60–90 km depth) appears to fit well with this geophysical model and strongly argues against the proposal of Fillerup et al. (2010), who suggested a relatively large scale (>100 km wide) lithospheric delamination, but involving also the dense lower crustal material. This scenario, i.e. asthenospheric upwelling beneath a 40 km continental crust as shown by their figure 3, would result in a more intense and presumably even silicic magmatism. Furthermore, the presence of peridotite xenoliths in the Perşani basalts (Vaselli et al., 1995) clearly implies that lithospheric mantle material exists beneath this area.

The seismic tomographic images of Popa et al. (2012) do not show a laterally continuous low-velocity anomaly in the sublithospheric mantle but rather a local one surrounded by higher velocity mantle material. The strongest low-velocity anomaly is between 25 and 45 km depth, i.e. in the lower crustal and crust–mantle boundary zones, and this can be followed down to 100 km depth. The seismic model of Popa et al. (2012) is consistent with our petrologic and petrogenetic results, i.e. localized asthenospheric mantle upwelling beneath the Perşani volcanic field. The reason for this might not be a large-scale lithospheric material delamination, but rather a far-field effect of the descending "cold material" beneath the Vrancea zone and reactivation of former tectonic lines. Seghedi et al. (2011) suggested a tear in the lower plate between the Moesian block and the European–Scythian plate, perpendicular to the strike of the orogen, along the Trotuş fault system that allowed the asthenosphere to flow around and into the tear. Stretching in the lithosphere caused by the downgoing slab beneath Vrancea and/or upwelling toroidal asthenospheric flow could initiate irregular thinning and formation of a narrow rupture at the base of the lithosphere northwest of the Vrancea zone. Upwelling of asthenospheric material into this narrow rupture (Fig. 12) could lead to partial melting and basaltic volcanism. Many alkali basalt volcanic fields close to orogenic areas show this localized, low-volume flux feature (e.g., Mediterranean region; Beccaluva et al., 2011; Jeju island volcanic field in Korea; Brenna et al., 2012; the Auckland volcanic field, New Zealand, Bebbington and Cronin, 2011) and this could imply the importance of the local tectonic structure and reactivation due to the far-field effect of the nearby, often near-vertical descending slab.

The geodynamic situation in the SE Carpathians appears to be still capable of further, but presumably still low-volume flux, volcanic activity (Szakács and Seghedi, 2013). The relative frequent earthquakes (Mw = 6.5 earthquakes each 10 years and Mw > 7 each 50 years; Cloetingh et al., 2004) in the Vrancea zone suggest the active descent of the cold material into the mantle causing a large concentration of strain (Wenzel et al., 1999). Recent seismic tomographic images (Popa et al., 2012) show vertically extended low velocity zones beneath Perşani that the authors attributed to possible magma accumulation. The extensional stress-field in this area and episodic reactivation of the normal faults (Gîrbacea et al., 1998) could have a primary role in controlling the rapid ascent of mafic magma batches. High-resolution geophysical investigations could help to refine the upper mantle structure beneath this complex area, whereas more detailed $^{40}Ar/^{39}Ar$ dating could help to constrain the temporal evolution of the volcanic activity.

Coexistence of alkaline basaltic and calc-alkaline volcanic rocks occurs in many places in the Mediterranean (Beccaluva et al., 2011; Harangi et al., 2006; Lustrino et al., 2011; Wilson and Bianchini, 1999). In addition, alkaline basalts and other silica-undersaturated mafic rocks can be found also in central and western Europe without associated calc-alkaline volcanic products (Lustrino and Wilson, 2007; Wilson and Downes, 1991). The composition of the alkaline basalts is consistent with derivation mostly from upwelling asthenopheric mantle as indicated by their low La/Nb ratio (<1; Fig. 13). A few alkaline basaltic volcanic fields in orogenic areas (e.g., Turkey, Etna-Hyblean, some volcanic fields in the Carpathian–Pannonian region) were fed by mafic magmas with similar composition as found in central and western Europe (Fig. 13). This means that the mantle source affected by subduction-related metasomatism was replaced effectively by OIB-type mantle domain (Beccaluva et al., 2011; Lustrino et al., 2011). In some cases (e.g., the Betic area, Sardinia, Veneto, Ustica island), including the Perşani area, the composition of the alkaline basalts differ slightly from the other regions and are characterized by lower La/Ba ratio and larger variation of La/Nb values. In these areas, it appears that the change in the mantle source was not so effective and the alkaline basaltic magmas were generated from a more heterogeneous mantle.

6. Conclusions

Combined bulk rock and mineral-scale investigations of the Perşani basalts in the southeast Carpathians led to the following main conclusions regarding the origin of the basaltic magmas:

(1) The studied mafic volcanic rocks (alkali basalts and silica-undersaturated hawaiites) have bulk rock compositions close to primary magmas. During magma evolution, olivine and spinel crystallized first as liquidus phases at 1300–1350 °C, followed by clinopyroxenes at about 1250 °C and 0.8–1.2 GPa.

(2) Trace element ratios and major element compositions of the bulk rocks suggest melt generation in an upwelling asthenospheric mantle at normal mantle potential temperature (1350–1420 °C; the lowest in the Pannonian Basin) in a melting column with initial

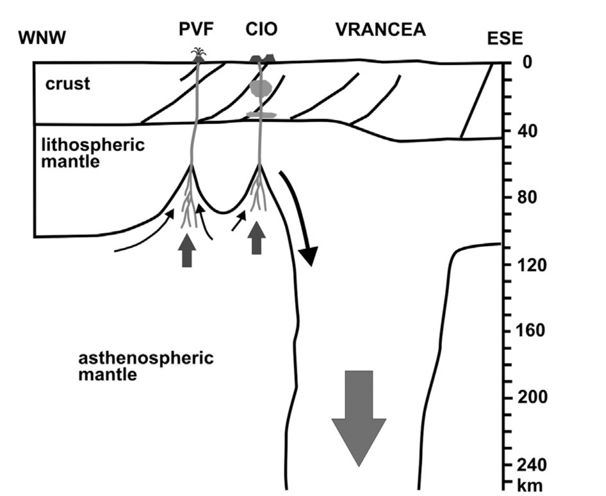

Fig. 12. Conceptual model for the origin of the volcanism in the Perşani Volcanic Field (PVF) and the Ciomadul (CIO) modifying the figure published by Seghedi et al. (2011). Local ruptures in the lower lithosphere could have formed due to the suction of the downgoing lithospheric slab beneath the nearby Vrancea Zone. Melt generation in the 60–95 km depth range can be explained by the upwelling asthenospheric mantle material into this voids.

Please cite this article as: Harangi, S., et al., Origin of basaltic magmas of Perşani volcanic field, Romania: A combined whole rock and mineral scale investigation, Lithos (2013), http://dx.doi.org/10.1016/j.lithos.2013.08.025

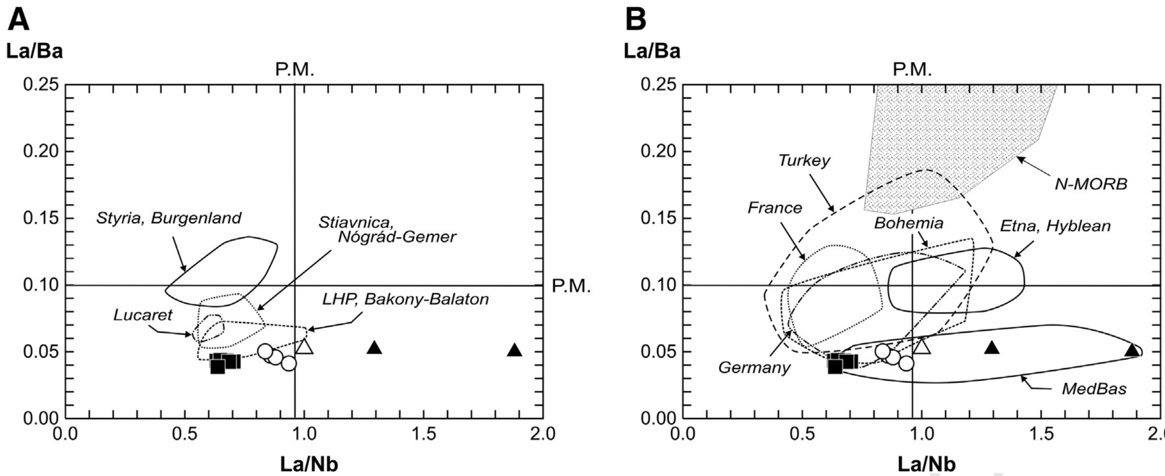

Fig. 13. La/Nb vs. La/Ba ratio diagrams (after Harangi, 2001b) for the alkali basalts found in the Mediterranean region and its surroundings. The compositional fields of the alkaline basalt areas from the Pannonian basin are from Embey-Isztin et al. (1993), Dobosi et al. (1995), Harangi et al. (1995), Tschegg et al. (2010), Ali and Ntaflos (2011), Jankovics et al. (2012) and Ali et al. (2013). MedBas refers to the alkaline basalt volcanic fields of the Betic area, Sardinia, Veneto and Ustica island. Symbols are explained in Fig. 3.
Reference data from the Mediterranean and the surrounding areas are from the database compiled by Lustrino and Wilson (2007).

melting depth of 85–90 km and final melting depth of about 60 km. This implies no thermal anomaly in the sublithospheric mantle and a relatively thin lithosphere beneath the Perşani area.

(3) The mantle source could be slightly heterogeneous, but is dominantly MORB-source, variously depleted peridotite, as shown by the composition of the olivines and spinels. Spinel Cr-number suggests two main coherent peridotite compositional groups that also characterize the whole sublithospheric mantle beneath the Pannonian basin. These two spinel groups correspond to the older and younger volcanic products, i.e. a change in the mantle source region can be invoked during the volcanic activity. This is detected also in the major and trace element data of the basalts. The younger basaltic magmas were generated by lower degree of melting, from a deeper and compositionally slightly different mantle source compared to the older ones. The mantle source character of the Perşani magmas is similar to many other alkaline basalt volcanic fields in the Mediterranean close to orogenic areas.

(4) The alkaline basalt magmas could penetrate the continental crust rapidly, within only 4–5 days, following about 1.3 years of heating of the lower lithosphere by the uprising magma. This ascent rate is consistent with the recent calculations for other localities in intra-continental setting (e.g., Tanzania, Mattsson, 2012 and central Pannonian basin, Jankovics et al., 2013).

(5) The alkaline basaltic volcanism in the Perşani volcanic field could be attributed to the formation of a narrow rupture in the lower lithosphere beneath this area, possibly as a far-field effect of the dripping of the dense continental lithospheric material beneath the Vrancea zone. A large-scale (>100 km wide) delamination of lithospheric material beneath this region is not consistent with the localized low-volume flux volcanism. Upper crustal extensional stress-field with reactivation of normal faults at the south-eastern margin of the Transylvanian basin could enhance the rapid ascent of the mafic magmas. The present geodynamic situation might be capable of leading to further volcanic activity in this area.

Acknowledgments

This research belongs to the study of the youngest volcanic activity in the Carpathian–Pannonian region, funded by the Hungarian National Science Foundation to SH (OTKA no. 68587) and supported also by a cooperative Hungarian–Austrian project (TÉT_10-1-2011-0694) on the origin of the basaltic volcanism in the Pannonian Basin. Discussion with Éva Jankovics and Balázs Kiss provided a continuous inspiration during this research. We thank Franz Kiraly for the careful help during the microprobe work in Vienna. Constructive comments provided by two anonymous reviewers as well as the helpful remarks given by Dejan Prelevic contributed significantly to improve the manuscript. We thank Hilary Downes for helping with the final English corrections.

Appendix A. Supplementary data

Supplementary data to this article can be found online at http://dx.doi.org/10.1016/j.lithos.2013.08.025.

References

Ali, S., Ntaflos, T., 2011. Alkali basalts from Burgenland, Austria: petrological constraints on the origin of the westernmost magmatism in the Carpathian–Pannonian Region. Lithos 121, 176–188.
Ali, S., Ntaflos, T., Upton, B.G.J., 2013. Petrogenesis and mantle source characteristics of Quaternary alkaline mafic lavas in the western Carpathian–Pannonian Region, Styria, Austria. Chemical Geology 337–338, 99–113.
Arai, S., 1994. Compositional variation of olivine-chromian spinel in Mg-rich magmas as a guide to their residual spinel peridotites. Journal of Volcanology and Geothermal Research 59, 279–293.
Balogh, K., Ebner, F., Ravasz, Cs, 1994. K/Ar alter tertiärer Vulcanite de südöstlischen Steiermark und des südlichen Burgenlands. In: Császár, G., Daurer, A. (Eds.), Jubiläumsschrift 20 Jahre Geologischen Zusammenarbeit Österreich-Ungarn Lobitzer, pp. 55–72.
Bannister, V., Roeder, P., Poustovetov, A., 1998. Chromite in the Paricutin lava flows (1943–1952). Journal of Volcanology and Geothermal Research 87 (1–4), 151–171.
Bebbington, M.S., Cronin, S.J., 2011. Spatio-temporal hazard estimation in the Auckland Volcanic Field, New Zealand, with a new event-order model. Bulletin of Volcanology 73, 55–72.
Beccaluva, L., Bianchini, G., Bonadiman, C., Coltorti, M., Milani, L., Salvini, L., Siena, F., Tassinari, R., 2007. Intraplate lithospheric and sub-lithospheric components in the Adriatic domain: nephelinite to tholeiite magma generation in the Paleogene Veneto Volcanic Province, Southern Alps. In: Beccaluva, L., Bianchini, G., Wilson, M. (Eds.), Cenozoic Volcanism in the Mediterranean AreaGeological Society of America, Special Paper 418, 131–152.
Beccaluva, L., Bianchini, G., Natali, C., Siena, F., 2011. Geodynamic control on orogenic and anorogenic magmatic phases in Sardinia and Southern Spain: inferences for the Cenozoic evolution of the western Mediterranean. Lithos 123, 218–224.
Bianchini, G., Beccaluva, L., Siena, F., 2008. Postcollisional and intraplate Cenozoic volcanism in the rifted Apennines/Adriatic domain. Lithos 101, 125–140.
Bradshaw, T.K., Hawkesworth, C.J., Gallagher, K., 1993. Basaltic volcanism in the Southern Basin and Range: no role for a mantle plume. Earth and Planetary Science Letters 116, 45–62.
Brenna, M., Cronin, S.J., Smith, I.E.M., Maas, R., Sohn, Y.K., 2012. How small-volume basaltic magmatic systems develop: a case study from the Jeju Island Volcanic Field, Korea. Journal of Petrology 53, 985–1018.

Chalot-Prat, F., Gîrbacea, R., 2000. Partial delamination of continental mantle lithosphere, uplift-related crust-mantle decoupling, volcanism and basin formation: a new model for the Pliocene–Quaternary evolution of the southern East-Carpathians, Romania. Tectonophysics 327, 83–107.
Ciulavu, D., Dinu, C., Szakács, A., Dordea, D., 2000. Neogene kinematics of the Transylvanian Basin (Romania). AAPG Bulletin 84, 1589–1615.
Cloetingh, S.A.P.L., Burov, E., Matenco, L., Toussaint, G., Bertotti, G., Andriessen, P.A.M., Wortel, M.J.R., Spakman, W., 2004. Thermo-mechanical controls on the mode of continental collision in the SE Carpathians (Romania). Earth and Planetary Science Letters 218, 57–76.
Cornea, I., Dragoescu, I., Popescu, M., Visarion, M., 1979. Harta miscarilor crustale verticale recente pe teritoriul R.S. România. Studii si Cercetari de Geologie, Geofizica, Geografie, Seria Geofizica 17, 3–17.
Costa, F., Cohmen, R., Chakraborty, S., 2008. Time scales of magmatic processes from modeling the zoning patterns of crystals. In: Putirka, K.D., Tepley III, F.J. (Eds.), Minerals, Inclusions and Volcanic Processes. Mineralogical Society of America & Geochemical Society, pp. 545–594.
Dérerova, J., Zeyen, H., Bielik, M., Salman, K., 2006. Application of integrated geophysical modeling for determination of the continental lithospheric thermal structure in the eastern Carpathians. Tectonics 25, TC3009. http://dx.doi.org/10.1029/2005TC001883.
Dick, H.J.B., Bullen, T., 1984. Chromian spinel as a petrogenetic indicator in abyssal and alpine-type peridotites and spatially associated lavas. Contributions to Mineralogy and Petrology 86 (1), 54–76.
Dobosi, G., Fodor, R.V., Goldberg, S.A., 1995. Late-Cenozoic alkali basalt magmatism in Northern Hungary and Slovakia: petrology, source compositions and relationship to tectonics. Acta Vulcanologica 7, 199–207.
Downes, H., Seghedi, I., Szakács, A., Dobosi, G., James, D.E., Vaselli, O., Rigby, I.J., Ingram, G.A., Rex, D., Pécskay, Z., 1995. Petrology and geochemistry of late Tertiary/Quaternary mafic alkaline volcanism in Romania. Lithos 35, 65–81.
Embey-Isztin, A., Downes, H., James, D.E., Upton, B.G.J., Dobosi, G., Ingram, G.A., Harmon, R.S., Scharbert, H.G., 1993. The petrogenesis of Pliocene alkaline volcanic rocks from the Pannonian Basin, Eastern Central Europe. Journal of Petrology 34, 317–343.
Fillerup, M.A., Knapp, J.H., Knapp, C.C., Raileanu, V., 2010. Mantle earthquakes in the absence of subduction? Continental delamination in the Romanian Carpathians. Lithosphere 2, 333–340.
Fitton, J.G., James, D., Kempton, P.D., Ormerod, D.S., Leeman, W.P., 1988. The role of lithospheric mantle in the generation of Late Cenozoic basic magmas in the western United States. Journal of Petrology (1), 331–349 (Special Volume).
Fitton, J.G., James, D., Leeman, W.P., 1991. Basic magmatism associated with Late Cenozoic extension in the Western United States: compositional variations in space and time. Journal of Geophysical Research 96, 13693–13711.
Gîrbacea, R., Frisch, W., 1998. Slab in the wrong place: lower lithospheric mantle delamination in the last stage of Eastern Carpathians subduction retreat. Geology 26, 611–614.
Gîrbacea, R., Frisch, W., Linzer, H.-G., 1998. Post-orogenic uplift induced extension: a kinematic model for the Pliocene to recent tectonic evolution of the Eastern Carpathians (Romania). Geologica Carpathica 49, 315–327.
Harangi, S., 2001a. Neogene to Quaternary volcanism of the Carpathian–Pannonian Region — a review. Acta Geologica Hungarica 44, 223–258.
Harangi, S., 2001b. Neogene magmatism in the Alpine–Pannonian Transition Zone — a model for melt generation in a complex geodynamic setting. Acta Vulcanologica 13, 25–39.
Harangi, S., 2012. Petrogenesis of the Late Miocene–Quaternary alkaline basalts in the Pannonian Basin, eastern-central Europe. In: Ārentsen, K., Németh, K., Smid, E. (Eds.), Abstract Volume of the Fourth International Maar Conference — Geoscience Society of New Zealand Miscellaneous Publication, 131A, pp. 37–38.
Harangi, S., Lenkey, L., 2007. Genesis of the Neogene to Quaternary volcanism in the Carpathian–Pannonian region: role of subduction, extension, and mantle plume. Geological Society of America Special Papers 418, 67–92.
Harangi, S., Vaselli, O., Tonarini, S., Szabó, C., Harangi, R., Coradossi, N., 1995. Petrogenesis of Neogene extension-related alkaline volcanic rocks of the Little Hungarian Plain Volcanic Field (Western Hungary). Acta Vulcanologica 7, 173–187.
Harangi, S., Downes, H., Seghedi, I., 2006. Tertiary–Quaternary subduction processes and related magmatism in the Alpine–Mediterranean region. In: Gee, D.G., Stephenson, R.A. (Eds.), European Lithosphere DynamicsGeological Society, London, Memoirs 32, 167–190.
Harangi, S., Molnár, M., Vinkler, A.P., Kiss, B., Jull, A.J.T., Leonard, A.G., 2010. Radiocarbon dating of the last volcanic eruptions of Ciomadul Volcano, southeast Carpathians, Eastern-Central Europe. Radiocarbon 52, 1498–1507.
Herzberg, C., 2011. Identification of source lithology in the Hawaiian and Canary Islands: implications for origins. Journal of Petrology 52, 113–146.
Herzberg, C., Asimow, P.D., 2008. etrology of some oceanic island basalts: PRIMELT2.XLS software for primary magma calculation. Geochemistry, Geophysics, Geosystems 9. http://dx.doi.org/10.1029/2008GC002057.
Hirose, K., Kushiro, I., 1993. Partial melting of dry peridotites at high pressures: determination of composition of melts segregated from peridotite using aggregate of diamonds. Earth and Planetary Science Letters 114, 477–489.
Horváth, F., Bada, G., Szafián, P., Tari, G., Ádám, A., Cloething, S., 2006. Formation and deformation of the Pannonian Basin. In: Gee, D.G., Stephenson, R.A. (Eds.), European Lithosphere DynamicsGeological Society London Memoirs 32, 191–207.
Ismail-Zadeh, A., Matenco, L., Radulian, M., Cloetingh, S., Panza, G., 2012. Geodynamics and intermediate-depth seismicity in Vrancea (the south-eastern Carpathians): current state-of-the art. Tectonophysics 530–531, 50–79.
Jankovics, M.É., Harangi, S., Kiss, B., Ntaflos, T., 2012. Open-system evolution of the Füzes-tó alkaline basaltic magma, western Pannonian Basin: constraints from mineral textures and compositions. Lithos 140–141, 25–37.
Jankovics, M.É., Dobosi, G., Embey-Isztin, A., Kiss, B., Sági, T., Harangi, S., Ntaflos, T., 2013. Origin and ascent history of unusually crystal-rich alkaline basaltic magmas from the western Pannonian Basin. Bulletin of Volcanology 75, 1–23.
Jurewicz, A.J.G., Watson, E.B., 1988. Cations in olivine, part 2: diffusion in olivine xenocrysts, with applications to petrology and mineral physics. Contributions to Mineralogy and Petrology 99, 186–201.
Kamenetsky, V.S., Crawford, A.J., Meffre, S., 2001. Factors controlling chemistry of magmatic spinel: an empirical study of associated olivine, Cr-spinel and melt inclusions from primitive rocks. Journal of Petrology 42, 655–671.
Kil, Y., Wendlandt, R.F., 2004. Pressure and temperature evolution of upper mantle under the Rio Grande Rift. Contributions to Mineralogy and Petrology 148, 265–280.
Klemme, S., 2004. The influence of Cr on the garnet–spinel transition in the Earth's mantle: experiments in the system MgO–Cr_2O_3–SiO_2 and thermodynamic modelling. Lithos 77, 639–646.
Köhler, T., Brey, G.P., 1990. Ca-exchange between olivine and clinopyroxene as a geothermobarometer calibrated from 2 to 60 kbar in primitive natural lherzolites. Geochimica et Cosmochimica Acta 54, 2375–2388.
Konečný, V., Kováč, M., Lexa, J., Šefara, J., 2002. Neogene evolution of the Carpatho-Pannonian region: an interplay of subduction and back-arc diapiric uprise in the mantle. EGU Stephan Mueller Special Publication Series, 1 105–123.
Kostopoulos, D.K., James, S.D., 1992. Parameterization of the melting regime of the shallow upper mantle and the effects of variable lithospheric stretching on mantle modal stratification and trace element concentrations in magmas. Journal of Petrology 33, 665–691.
Koulakov, I., Zaharia, B., Enescu, B., Radulian, M., Popa, M., Parolai, S., Zschau, J., 2010. Delamination or slab detachment beneath Vrancea? New arguments from local earthquake tomography. Geochemistry, Geophysics, Geosystems 11. http://dx.doi.org/10.1029/2009GC002811.
Langmuir, C., Klein, E., Plank, T., 1992. Petrological systematics of mid-ocean ridge basalts: constraints on melt generation beneath ocean ridges. AGU Monograph 71, 183–280.
Lasaga, A.C., 1998. Kinetic Theory in the Earth Sciences. Princeton University Press.
Lee, C.-T., Luffi, P., Plank, T., Dalton, H., Leeman, W.P., 2009. Constraints on the depths and temperatures of basaltic magma generation on Earth and other terrestrial planets using new thermobarometers for mafic magmas. Earth and Planetary Science Letters 279, 20–33.
Lustrino, M., 2005. How the delamination and detachment of lower crust can influence basaltic magmatism. Earth-Science Reviews 72, 21–38.
Lustrino, M., Wilson, M., 2007. The circum-Mediterranean anorogenic Cenozoic igneous province. Earth-Science Reviews 81, 1–65.
Lustrino, M., Duggen, S., Rosenberg, C.L., 2011. The central-western Mediterranean: anomalous igneous activity in an anomalous collisional tectonic setting. Earth-Science Reviews 104, 1–40.
Martin, U., Németh, K., 2004. Mio/Pliocene Phreatomagmatic Volcanism in the Western Pannonian Basin. Geological Institute of Hungary, Budapest (193 pp.).
Martin, M., Wenzel, F., CALIXTO Working Group, 2006. High-resolution teleseismic body wave tomography beneath SE Romania: II. Imaging of a slab detachment scenario. Geophysical Journal International 164, 579–595.
Maţenco, L., Bertotti, G., Leever, K., Cloetingh, S., Schmid, S.M., Tărăpoancă, M., Dinu, C., 2007. Large-scale deformation in a locked collisional boundary: interplay between subsidence and uplift, intraplate stress, and inherited lithospheric structure in the late stage of the SE Carpathians evolution. Tectonics 26. http://dx.doi.org/10.1029/2006TC001951.
Mattsson, H.B., 2012. Rapid magma ascent and short eruption durations in the Lake Natron–Engaruka monogenetic volcanic field (Tanzania): a case study of the olivine melilititic Pello Hill scoria cone. Journal of Volcanology and Geothermal Research 247–248, 16–25.
McDonough, W.F., Sun, S.S., 1995. The composition of the Earth. Chemical Geology 120, 223–253.
McKenzie, D., O'Nions, R.K., 1991. Partial melt distributions from inversion of rare-earth element concentrations. Journal of Petrology 32, 1021–1091.
Németh, K., 2010. Monogenetic volcanic fields: origin, sedimentary record, and relationship with polygenetic volcanism. Geological Society of America Special Papers 470, 43–66.
Niu, Y., Wilson, M., Humphreys, E.R., O'Hara, M.J., 2011. The origin of intra-plate ocean island basalts (OIB): the lid effect and its geodynamic implications. Journal of Petrology 52, 1443–1468.
Panaiotu, C.G., Pécskay, Z., Hambach, U., Seghedi, I., Panaiotu, C.E., Tetsumaru, I., Orleanu, M., Szakács, A., 2004. Short-lived Quaternary volcanism in the Persani Mountains (Romania) revealed by combined K–Ar and paleomagnetic data. Geologica Carpathica 55, 333–339.
Panaiotu, C.G., Jicha, B.R., Singer, B.S., Tugui, A., Seghedi, I., Panaiotu, A.G., Necula, C., 2013. $^{40}Ar/^{39}Ar$ chronology and paleomagnetism of Quaternary basaltic lavas from the Perşani Mountains (East Carpathians). Physics of the Earth and Planetary Interiors 221, 1–24.
Pécskay, Z., Edelstein, O., Seghedi, I., Szakacs, A., Kovacs, M., Crihan, M., Bernad, A., 1995. K–Ar datings of Neogene–Quaternary calc-alkaline volcanic rocks in Romania. Acta Vulcanologica 7, 53–61.
Pécskay, Z., Lexa, J., Szakács, A., Seghedi, I., Balogh, K., Konečný, V., Zelenka, T., Kovacs, M., Póka, T., Fülöp, A., Márton, E., Panaiotu, C., Cvetković, V., 2006. Geochronology of Neogene–Quaternary magmatism in the Carpathian arc and intra-Carpathian area: a review. Geologica Carpathica 57, 511–530.
Pilet, S., Baker, M.B., Stolper, E.M., 2008. Metasomatized lithosphere and the origin of alkaline lavas. Science 320, 916–919.
Popa, M., Radulian, M., Szakács, A., Seghedi, I., Zaharia, B., 2012. New seismic and tomography data in the southern part of the Harghita Mountains (Romania, southeastern Carpathians): connection with recent volcanic activity. Pure and Applied Geophysics 169 (9), 1557–1573.

Putirka, K.D., 2008. Thermometers and barometers for volcanic systems. In: Putirka, K.D., Tepley, F. (Eds.), Reviews in Mineralogy and Geochemistry 69, 61–120.

Putirka, K.D., Johnson, M., Kinzler, R., Walker, D., 1996. Thermobarometry of mafic igneous rocks based on clinopyroxene–liquid equilibria, 0–30 kbar. Contributions to Mineralogy and Petrology 123, 92–108.

Putirka, K.D., Perfit, M., Ryerson, F.J., Jackson, M.G., 2007. Ambient and excess mantle temperatures, olivine thermometry, and active vs. passive upwelling. Chemical Geology 241, 177–206.

Ren, Y., Stuart, G.W., Houseman, G.A., Dando, B., Ionescu, C., Hegedűs, E., Radovanovic, S., Shen, Y., South Carpathian Project Working Group, 2012. Upper mantle structures beneath the Carpathian–Pannonian region: Implications for the geodynamics of continental collision. Earth and Planetary Science Letters 349–350, 139–152.

Rhodes, J.M., Lofgren, G.E., Smith, B.P., 1979. One atmosphere melting experiments on ilmenite basalt 12008. Proc 10th Lunar Sci. Conf, pp. 407–422.

Roeder, P.L., 1994. Chromite: from the fiery rain of chondrules to the Kilauea Iki lava lake. The Canadian Mineralogist 32, 729–746.

Roeder, P.L., Emslie, R.F., 1970. Olivine–liquid equilibrium. Contributions to Mineralogy and Petrology 29, 275–289.

Roeder, P.L., Poustovetov, A., Oskarsson, N., 2001. Growth forms and composition of chromian spinel in MORB magma: diffusion-controlled crystallization of chromian spinel. Canadian Mineralogist 39, 397–416.

Roeder, P.L., Thornber, C., Poustovetov, A., Grant, A., 2003. Morphology and composition of spinel in Pu'u 'O'o lava (1996–1998), Kilauea volcano, Hawaii. Journal of Volcanology and Geothermal Research 123, 245–265.

Roeder, P., Gofton, E., Thornber, C., 2006. Cotectic proportions of olivine and spinel in olivine-tholeiitic basalt and evaluation of pre-eruptive processes. Journal of Petrology 47, 883–900.

Rudnick, R.L., Fountain, D.M., 1995. Nature and composition of the continental crust: a lower crustal perspective. Reviews of Geophysics 33, 267–309.

Sakuyama, T., Ozawa, K., Sumino, H., Nagao, K., 2009. Progressive melt extraction from upwelling mantle constrained by the Kita–Matsuura Basalts in NW Kyushu, SW Japan. Journal of Petrology 50, 725–779.

Scarrow, J.H., Cox, K.G., 1995. Basalts generated by decompressive adiabatic melting of a mantle plume: a case study from the Isle of Skye, NW Scotland. Journal of Petrology 36, 3–22.

Seghedi, I., Downes, H., 2011. Geochemistry and tectonic development of Cenozoic magmatism in the Carpathian–Pannonian region. Gondwana Research 20, 655–672.

Seghedi, I., Szakács, A., 1994. The Upper Pliocene–Pleistocene effusive and explosive basaltic volcanism from the Perşani Mountains. Romanian Journal of Petrology 76, 101–107.

Seghedi, I., Downes, H., Szakacs, A., Mason, P.R.D., Thirlwall, M.F., Rosu, E., Pecskay, Z., Marton, E., Panaiotu, C., 2004a. Neogene–Quaternary magmatism and geodynamics in the Carpathian–Pannonian region: a synthesis. Lithos 72, 117–146.

Seghedi, I., Downes, H., Vaselli, O., Szakács, A., Balogh, K., Pécskay, Z., 2004b. Post-collisional Tertiary–Quaternary mafic alkalic magmatism in the Carpathian–Pannonian region: a review. Tectonophysics 393, 43–62.

Seghedi, I., Maţenco, L., Downes, H., Mason, P.R.D., Szakács, A., Pécskay, Z., 2011. Tectonic significance of changes in post-subduction Pliocene–Quaternary magmatism in the south east part of the Carpathian–Pannonian Region. Tectonophysics 502, 146–157.

Shukuno, H., Arai, S., 1999. Olivine–chromian spinel compositional relationships of the Cenozoic alkali basalts from Southwest Japan: implication for their mantle restites. Journal of Petrology, Mineralogy and Economic Geology 94, 120–140.

Smith, D.R., Leeman, W.P., 2005. Chromian spinel–olivine phase chemistry and the origin of primitive basalts of the southern Washington Cascades. Journal of Volcanology and Geothermal Research 140, 49–66.

Smith, I.E.M., Blake, S., Wilson, C.J.N., Houghton, B.F., 2008. Deep-seated fractionation during the rise of a small-volume basalt magma batch: Crater Hill, Auckland, New Zealand. Contributions to Mineralogy and Petrology 155, 511–527.

Sobolev, A.V., Hofmann, A.W., Kuzmin, D.V., Yaxley, G.M., Arndt, N.T., Chung, S.-L., Danyushevsky, L.V., Elliott, T., Frey, F.A., Garcia, M.O., Gurenko, A.A., Kamenetsky, V.S., Kerr, A.C., Krivolutskaya, N.A., Matvienkov, V.V., Nikogosian, I.K., Rocholl, A., Sigurdsson, I.A., Sushchevskaya, N.M., Teklay, M., 2007. The amount of recycled crust in sources of mantle-derived melts. Science 316, 412–417.

Sperner, B., Lorenz, F., Bonjer, K., Hettel, S., Muller, B., Wenzel, F., 2001. Slab break-off – abrupt cut or gradual detachment? New insights from the Vrancea Region (SE Carpathians, Romania). Terra Nova 13, 172–179.

Stormer, J.C., 1973. Calcium zoning in olivine and its relationship to silica activity and pressure. Geochimica et Cosmochimica Acta 37, 1815–1821.

Szabó, C., Harangi, S., Csontos, L., 1992. Review of Neogene and Quaternary volcanism of the Carpathian–Pannonian region. Tectonophysics 208, 243–256.

Szakács, A., Seghedi, I., 2013. The relevance of volcanic hazard in Romania: is there any? Environmental Engineering and Mining Journal 12, 125–135.

Takahashi, E., Kushiro, I., 1983. Melting of a dry peridotite at high pressures and basalt magma genesis. American Mineralogist 68, 859–879.

Tschegg, C., Ntaflos, Th., Kiraly, F., Harangi, S., 2010. High temperature corrosion of olivine phenocrysts in Pliocene basalts from Banat, Romania. Austrian Journal of Earth-Sciences 103 (1), 101–110.

Valentine, G.A., Perry, F.V., 2007. Tectonically controlled, time-predictable basaltic volcanism from a lithospheric mantle source (central Basin and Range Province, USA). Earth and Planetary Science Letters 261, 201–216.

Vaselli, O., Downes, H., Thirlwall, M.F., Dobosi, G., Coradossi, N., Seghedi, I., Szakács, A., Vannucci, R., 1995. Ultramafic xenoliths in Plio-Pleistocene alkali basalts from the Eastern Transylvanian Basin: depleted mantle enriched by vein metasomatism. Journal of Petrology 36, 23–53.

Wang, K., Plank, T., Walker, J.D., Smith, E.I., 2002. A mantle melting profile across the Basin and Range, SW USA. Journal of Geophysical Research: Solid Earth 107 (B1) (ECV 5-1-ECV 5-21.

Wenzel, F., Lorenz, F., Sperner, B., Oncescu, M.C., 1999. Seismotectonics of the Romanian Vrancea area. In: Wenzel, F., Lungu, D., Novak, O. (Eds.), Vrancea Earthquakes: Tectonics. Hazard and Risk Mitigation. Kluwer Academic Publishers, Dordrecht, pp. 15–26.

Wijbrans, J., Németh, K., Martin, U., Balogh, K., 2007. $^{40}Ar/^{39}Ar$ geochronology of Neogene phreatomagmatic volcanism in the western Pannonian Basin, Hungary. Journal of Volcanology and Geothermal Research 164, 193–204.

Wilson, M., Bianchini, G., 1999. Tertiary–Quaternary magmatism within the Mediterranean and surrounding regions. In: Durand, B., Jolivet, L., Horváth, F., Séranne, M. (Eds.), The Mediterranean Basins: Tertiary Extension Within the Alpine OrogenGeological Society London Special Publication 156, 141–168.

Wilson, M., Downes, H., 1991. Tertiary–Quaternary extension-related alkaline magmatism in Western and Central Europe. Journal of Petrology 32, 811–849.

Wortel, M.J.R., Spakman, W., 2000. Subduction and slab detachment in the Mediterranean–Carpathian region. Science 290, 1910–1917.

Please cite this article as: Harangi, S., et al., Origin of basaltic magmas of Perşani volcanic field, Romania: A combined whole rock and mineral scale investigation, Lithos (2013), http://dx.doi.org/10.1016/j.lithos.2013.08.025